SYMMETRIC AND ASYMMETRIC CRACK DEVELOPMENT IN TUBULAR T-JOINTS

SAMUEL PARANAVITANA

SYMMETRIC AND ASYMMETRIC CRACK DEVELOPMENT IN TUBULAR T - JOINTS

by

© *Samuel Paranavitana*

A thesis submitted to the School of Graduate Studies
in partial fulfilment of
the requirements for the degree
of
Master of Engineering

Faculty of Engineering & Applied Science
Memorial University of Newfoundland
January 1996

St. John's Newfoundland Canada

ISBN 0-612-13938-7

To those who gave me all the encouragement

especially my wife, Tara

Acknowledgement

I would like to take this opportunity to thank the following people for their support and encouragement throughout my Master's program.

Dr. J.J. Sharp, Dean of Graduate Studies, who cleared the way and made it possible for me to pursue my goal of obtaining a Master's degree.

Dr. A.S.J. Swamidas, Supervisor, mentor and friend, whose patient guidance and financial support made it possible to pursue my degree with a single minded purpose and determination.

Dr. D.I. Nwosu for taking time, out of his busy schedule to teach me all about the finite element package - "Abaqus", the program and its application to my work.

The Encon Insurance Group for the Encon Endowment, which I was privileged to receive for the year 1994-1995.

The Personnel at the C-CAE for their cooperation in computer related problems.

Finally, I would like to thank my wife and those who cared, for their unstinted support.

Abstract

Although many studies on the fatigue behaviour of tubular T-joints have been carried out thus far, the present study is done with the view to evaluating the total fatigue life of a joint in the presence of an asymmetric crack, using the principles of fracture mechanics. The studies made so far have only analyzed symmetric cracking, which does not generally occur during fatigue cracking, since it is assumed that the cracks at both the hot spot regions grow at the same rate. Also very few studies address the issue of crack initiation life in tubular T-joints. D.I. Nwosu (1993) used the stress-strain approach using the Manson-Coffin equation, to evaluate the initiation life. The elastic life component was used to determine the coefficients. In this study the author has used both lives (plastic strain life, as well as elastic strain life) to determine the coefficients used in the equation. The experimental results reported by Iida [1987] on tubular joints have been used to determine them. The range of obtained coefficients check with the prescribed limits given in earlier studies. The purpose of the study was to use and compare the results of the numerical model in verifying and correlating the experimental investigation of the tubular T-joints, which is being carried out in the Strength Laboratory of Faculty of Engineering, Memorial University.

The line spring element was used to model the crack; the reason being that the other known method, viz., that of using singular three dimensional elements would render the

problem impractical in the light of computer time and memory space available in the Faculty of Engineering. Using the stress intensity factors obtained from the line spring model, the through-thickness crack propagation life was obtained using Paris' law. While the crack initiation compared very well with the experimental value, the crack propagation life compared only favourably with the experimental value. The procedure required to improve the computed crack propagation life is given in the discussion of results.

Contents

List of Figures

List of Symbols

a	Crack depth
$\mathbf{a}_i^e$	Degrees of freedom at the i^{th} node of an element
a_0	Deepest point in a semi-elliptical crack
B	Strain shape function matrix
b	Fatigue strength component
C	Crack growth constant, Paris law
c	Index denoting components expressed in curvilinear coordinates
c	Fatigue ductility coefficient
D'	Elasticity matrix
D	Chord diameter
d	Brace diameter
E	Modulus of elasticity
G	Shear modulus
FEM	Finite element method

$\mathbf{J}$	Jacobian matrix
$\frac{da}{dN}$	Crack growth rate
K_I	Mode I stress intensity factor
K_{II}	Mode II stress intensity factor
K_{III}	Mode III stress intensity factor
ΔK	Stress intensity factor range
K'	Cyclic strength coefficient
k	Shear correction factor
L	Chord length
l	Brace length from chord surface
N_i	Shape function at node i
N_f	Fatigue crack initiation life (cycles)
N_p	Fatigue crack propagation life (cycles)
N_T	Total fatigue life (cycles)
n'	Cyclic strain hardening exponent
p	Tensor index
$\mathbf{S}$	Element property matrix

SCF	Stress concentration factor
SIF	Stress intensity factor
T	Chord thickness
t	Brace thickness
σ_f'	Fatigue strength coefficient
U	Displacement matrix
u_i, v_i, w_i	Displacements in the global x, y, z directions at node i
$\mathbf{V}_{1i}$, $\mathbf{V}_{2i}$, $\mathbf{V}_{3i}$	Vectors along the nodal coordinate axes
$\mathbf{v}_{1i}$, $\mathbf{v}_{2i}$, $\mathbf{v}_{3i}$	Unit vectors along the nodal coordinate axes
X	Position vector matrix
x, y, z	Global coordinate system
x', y', z'	Local coordinate system
α	2L/D
α_i, β_i	Rotations of normal at node i
β	d/D
γ	D/2T
ξ, η, ζ	Curvilinear coordinate set

θ	Cosine matrix of the local coordinate system
θ	Rotation
δ	Displacement
τ	Thickness ratio
τ	Shear stress

Chapter 1

1 Introduction

1.1 Background

What we identify as fatigue failure today was first analyzed in great detail by Wöhler [Almar-Næss (1985)], in his pursuit of a cause for railway axles to fail well below the then design load. This phenomenon has been observed in other structures as well, although it was not until the subject of fracture mechanics was well developed that it was possible to have a clearer understanding of it.

Steel offshore structures are fabricated by welding together various tubular components, and experience fluctuating loads in service; hence fatigue is a factor to reckon with in the design of the structure. The fluctuating loads could be attributed to several sources such as wave, wind, and current loads, in addition to the fluctuating deck loads. These steel frame type structures are invariably fabricated from tubular members that are welded together externally. The abrupt changes in geometry give rise to stress concentrations in the region, and are also likely to act as crack initiation sites. It is clear therefore that in designing the structure, the joint would have to be designed for fatigue strength. The traditional, design based on S/N curves, requires only a knowledge of the hot-spot stresses and strains and does not take into account the presence of initial flaws.

The advantage of using the fracture mechanics approach is that an initial crack which grows, serves as a critical parameter in estimating the useful life of the component; such a phenomenon is disregarded in the traditional approach. The fracture mechanics design methodology assumes that a crack exists at a critical location and advances as the stress intensity changes due to a changing load. The stress intensity factor depends upon the applied load, crack depth and the geometry of the joint. It is assumed that the stress intensity factor in the crack region varies linearly as a function of the nominal hot-spot stress, which in turn is a function of the applied nominal stress on the joint. It is this method that has been used in this study.

The theoretical stress at the tip of a crack is characterised by the stress intensity factor. While a closed form solution is possible for simple geometries, it is not possible to derive a closed form solution for a complex geometry such as a tubular T-joint. Several techniques have been developed to overcome such difficulties of which a numerical technique is one such and is an approximate method. In this study the finite element method is used to determine the stress intensity factors numerically, using the "ABAQUS" finite element software package.

Crack growth consist of two phases, an initiation stage and a propagation stage. While the initiation life cannot be estimated by the use of finite element method, the propagation life can be estimated by such means. The initiation life has been estimated using the experimental data, obtained for several T-joints and the nominal hot-spot

strain, obtained from the finite element analysis, and is based on the low cycle strain life method. The crack propagation life has been estimated using Paris' equation.

1.2 Scope of study

The objectives of this study are threefold. The principal reason is that no studies have been done on stress distribution and fatigue life estimation in tubular T-joints for asymmetric crack growth as the governing feature. In addition far the crack initiation life has not been included in a proper manner in the fatigue life calculations of tubular T-joints, although it has been the object of study by many. In the present study, the author has used experimental data obtained by Iida (1987) to compute the initiation life of the tubular T-joint.

This finite element model also served as a design model for computing the load to be applied on the tubular T-joint for the experimental work currently being done towards the Ph.D. thesis work of a fellow graduate student (Ms. Cheng Shumin). Fig. 1.1 on page five shows the tubular T-joint that was used in the experiment.

1.3 Organization of the thesis

The layout of the thesis is, as described below. This study emphasizes in the main, the use of the finite element method for fatigue life assessment of a tubular T-joint subjected to axial tensile load at the brace.

Chapter two covers the literature concerning the development of the finite element method in the realm of fracture mechanics, and its application to tubular T-joints, especially the line-spring element. It also covers the theoretical developments in the field of fracture mechanics. Chapter three deals with the theoretical basis and the development of the degenerated isoparametric element, which has been used to model the shell structure; the approximations made and the advantages of using a degenerated shell element have also been outlined. Chapter four covers: i) Description of the modelling procedure; ii) Ways in which the accuracy of the model was checked; iii) Stress patterns around the weld toe, and their variations as the crack front advanced through the thickness and along the weld toe region; and iv) Variations in the SIF's and their physical significance.

Chapter five discusses the initiation and propagation lives and the method by which the initiation life was derived from experimental data. It also discusses the differences between computed and experimental data, the likely causes, and the methods by which the values could be reconciled. Chapter six gives the conclusions drawn from the study as well as areas of further interest.

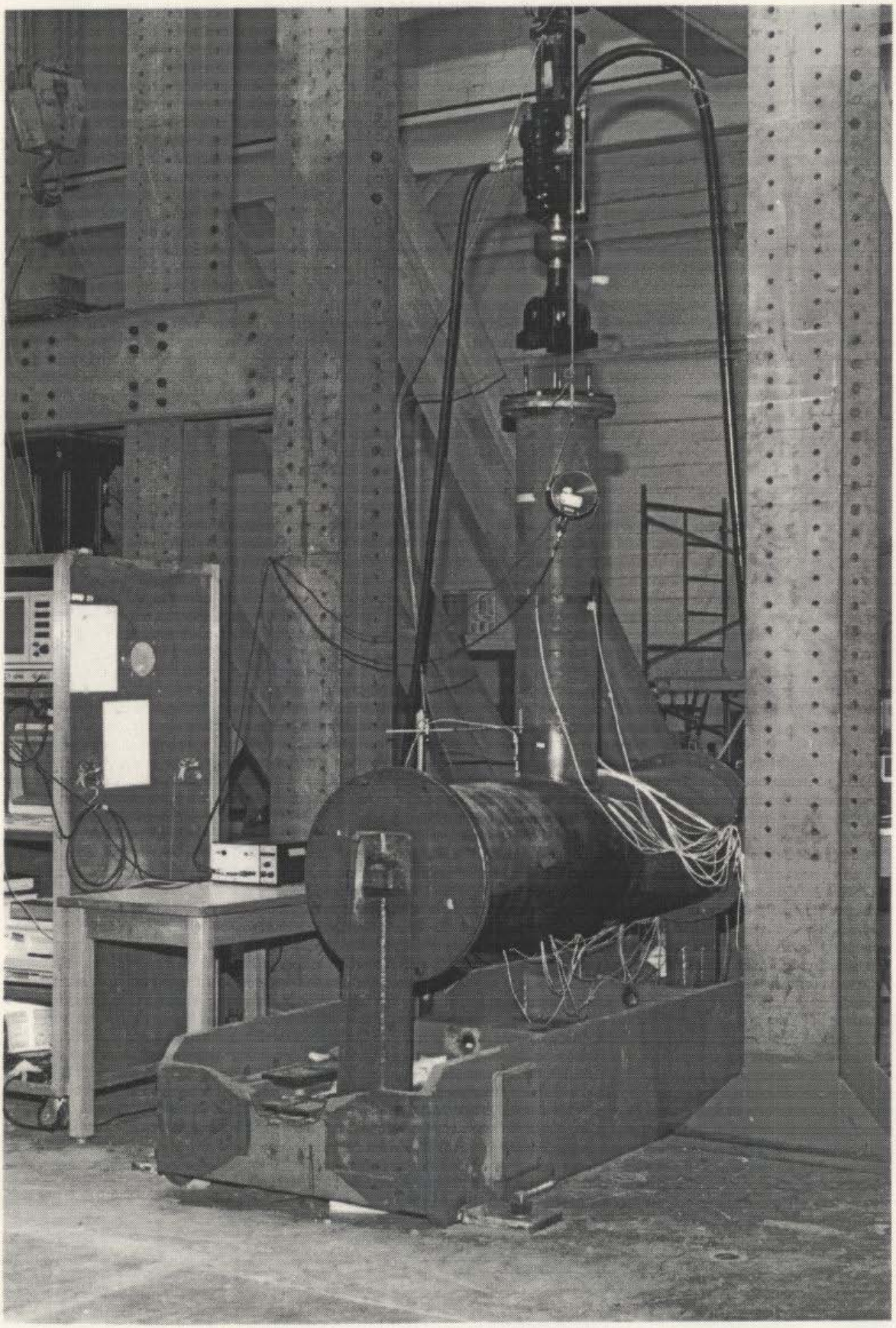

Fig. 1.1 Tubular T-joint

Chapter 2

Literature Review

2 Introduction

Fixed offshore structures are fabricated from tubular steel members. Such sections are well suited to being used as structural members in offshore structures, for several reasons. The section has a very low drag coefficient and the same bending stiffness in all directions perpendicular to its axis; it also has good torsional rigidity and is insensitive to lateral load directions. Although the tubular section itself is less prone to stress concentrations, the interconnections and joints which are usually welded, present structural discontinuities that give rise to high stress concentrations. The integrity of such structural connections is critically dependent on the behaviour of the component welded joints which resist the dynamic forces of wind, wave and currents and the topside loading.

It has been established that the initial flaw or imperfection present in the structure, which could be the result of the process of manufacture, fabrication, or usage, propagates under fatigue loading and spreads along the intersection before it penetrates through the thickness and causes failure of the joint. The complex lay-out of such a joint precludes a precise mathematical derivation of the stress and strain fields in and

around the weld. To study the behaviour of deformation and failure of the joint, engineers have developed experimental as well as analytical methods. Two methods of fatigue life evaluation of tubular joints are currently used in the offshore industry. The first is the hot spot stress - S/N method - which is widely used in design procedure; the second is the fracture mechanics method. Details of the two methods are given in the subsequent sections of this study.

The principles of fracture mechanics and the finite element method have been successfully used to some degree of sophistication, in analyzing the stress fields around a complex and cracked tubular joint. The recent advances in computer technology have made the application of numerical techniques a viable alternative to analytical and experimental methods, which could be prohibitive under certain circumstances. Notably, the finite element method has been well developed to model a region with the attributes of a crack, towards analysis. The pertinent literature available in this area of study are reviewed in this chapter, to understand the state-of-the-art developments in the analysis of fatigue and fracture of tubular T-joints.

2.1 Hot-Spot - S/N Approach to Fatigue Life Evaluation

It is now known that a low fatigue strength in a welded joint could be traced to the presence of stress raisers or stress concentrations around the welded regions of a tubular joint. Thus, a proper design against fatigue failure would take into account the stress concentration factors and the corresponding stresses in the calculation of the

fatigue life of a welded tubular joint. The stress distributions at the joint are very complex and are dependent on, the nature of the loading, and the geometry of the joint. In design work, welded joints are divided into classes, each of which with its characteristic design data. For e.g., all tubular joints fall into class "T". The class is dependent upon the geometrical arrangement of the joint, the direction of fluctuating stresses, and the method of fabrication and inspection [Almar-Næss (1985)]. The locations where the highest stresses occur are called *hot spots*. In the case of a tubular joint, *the stress concentration factor* (SCF) is defined as the ratio of the hot spot stress σ_{max} to the nominal stress σ_N in the brace; hence it can be looked upon as a scaling factor of the nominal stress.

$$SCF = \frac{\sigma_{max}}{\sigma_N} \tag{2.1}$$

Stress concentration factors may be determined by various methods, viz., analytical, computational, and experimental. Several parametric formulae for stress concentration factors have been derived. The earliest stress concentration factor formulae covering simple tubular joints under tensile loading were formulated by Beale and Toprac (1967). At present, the frequently used equations are attributed to Kuang et. al. (1975), Wordsworth and Smedley (1978), Underwater Engineering Group - UEG (1985), Efthymiou and Durkin (1988) and Hellier et. al. (1990b).

Kuang et. al. (1975) derived formulae for non-reinforced T, K, and TK joints, using FE models, which did not include the effects of the weld. Efthymiou and Durkin

(1985) presented parametric equations for T, Y, and K joints, having analyzed 150 FE models using three dimensional shell elements with the weld influence considered. The parametric formulae, derived by the various researchers just noted, differ from one another, which could be due to the model idealisations and the type and size of finite elements used. A notable drawback in the derivations is the fact that the influence of inherent defects and residual stresses are not considered. Although an offshore structure is fabricated carefully to prevent local distortion and/or cracking, routine inspection of the structure during service would reveal the presence of cracks; hence a proper analysis of tubular joints would require the use of the fracture mechanics approach.

The stress concentration factors are basically related to the degree of ovalisation of the chord section under the action of the brace loads. Since the stress concentration factor depends on the type of joint and the loading, it must be verified that the formula, which is used to determine the stress concentration factor, is for a joint that represents the physical behaviour of the joint under review. The parametric quantities used for the stress concentration factor are given below. Fig. 2.1 shows the geometrical quantities.

Diameter ratio	$\beta=d/D$,	Chord stiffness	$\gamma=D/2T$
Wall thickness ratio	$\tau=t/T$,	Gap diameter	$p=g/D$
Chord length	$\alpha=L/D$,	Brace inclination angle	$=\theta$

The geometrical parameters of the chord are indicated in simple letters while

those of the brace are referred to in capital letters.

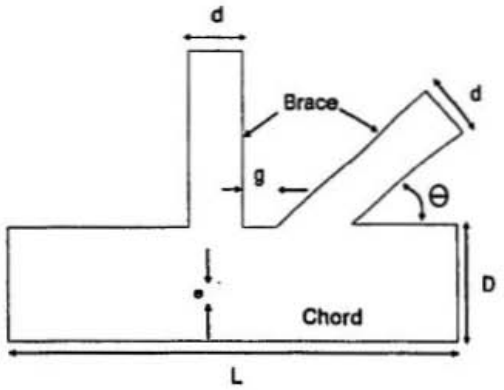

Fig. 2.1 Tubular joint symbols

The generalised form of the parametric equation for the stress concentration factor is given by:

$$SCF = C\alpha^{n1}\,\beta^{n2}\,\tau^{n3}\,\gamma^{n4}\,p^{n5}\,\sin^{n6}\theta \qquad (2.2)$$

where C is a constant, and the parametric quantities are defined as above; n1, n2, n3, n4, n5, n6 are exponents and θ is the intersection angle between members. Dover and Dharmavasan (1982) have derived simple interpolation functions for each mode of loading, from which the coefficients for stress concentration factors could be determined. Stress concentration factors may be obtained from tests on full scale steel joints, small scale acrylic models or finite element analyses, but for most design and re-certification work, the stress concentration factors are estimated using parametric equations. Dover et. al. (1991) analyzed the statistical variability of the equations formulated by Kuang et. al. (1975), Efthymiou and Durkin (1988), Wordsworth and

Smedley (1978), Underwater Engineering Group-UEG (1985), and Hellier et. al. (1990). They used a steel joint database and concluded that the then available database, while being adequate for some categories of tubular joints, is insufficient for many.

Having determined the stress concentration factors and the corresponding nominal stresses, the hot spot stress of any joint could be evaluated. In the hot spot - S/N method, the expected fatigue life is calculated first by locating the pre-determined hot spot stress ranges under the given varying cyclic wave loadings, which are then located on the S-N diagram (obtained from experiments) to determine the permissible number of cycles for each of the stress ranges. The basic S/N curves are obtained from a statistical analysis of experimental data and is given in a log-log plot with the stress range $\Delta\sigma$ on the vertical axis and the number of cycles to failure N_f on the horizontal axis. The fatigue life is then calculated using a damage summation law, e.g., the Miner-Palmgren formula:

$$D = \sum_{i=1}^{k} \frac{n_i}{N_i} \tag{2.3}$$

where,

k = No. of stress ranges

D is the accumulated damage due to varying stress cycles

n_i = No. of stress cycles in a stress block i with a constant stress range $\Delta\sigma_i$ and

N_i = No. of cycles to failure at a constant stress range $\Delta\sigma_i$.

Fatigue design of welded structures is based on constant amplitude S/N data.

However an offshore structure will experience a loading that is stochastic in nature. The development of fatigue damage under stochastic loading is termed cumulative damage. Of the several theories that can be found for calculating cumulative damage, the Miner's summation is much simpler and conforms with the fracture mechanics approach. The assumption in the Miner summation is that the damage on the structure per load cycle is constant at a given stress range and is D=1/N, where N is the constant amplitude endurance at the given stress range. In a constant amplitude test, the failure criterion is $D_f \geq 1$ [Almar-Næss 1985]. An accurate estimate of stress distribution at a tubular joint can be obtained only by finite element analysis or by strain gauge measurements. For practical applications, parametric formulae are needed to calculate the stress concentration factors or influence coefficients under single modes of loading. The disadvantage of the method is that any defect or imperfection which can be considered to shorten the life of the structure is not considered in the calculation. It gives us only a conservative estimate of the number of single mode cycles and is therefore a pass or fail criterion; the method cannot be used to compute the residual life of a component in service.

2.2 Fracture Mechanics Approach to Fatigue Life Evaluation

The discipline known as fracture mechanics was developed to explain failures due to ductile or brittle fracture, which couldn't be reconciled with the then conventional design criteria available at that period. The phenomenon of fracture of solids is complicated and depends on a variety of factors, which include microscopic

and macroscopic imperfections where the fracture initiates or grows. The study of the process of fracture depends at the level it is observed. At one extreme, fracture is concerned with the rupture of bonds, which calls for a knowledge of quantum mechanics to explain the phenomena. At the other extreme the material is considered to be a homogenous continuum, which calls for the application of continuum mechanics and classical thermodynamics to evaluate observed phenomena. The analysis of fracture at an intermediate level involves the movement of dislocations, slip bands etc. Hence the study of fracture is interdisciplinary and can be analyzed at three levels; atomic, microscopic, and the continuum. Here it is approached at the continuum level.

Central to the subject of fracture mechanics is the assumption that all materials contain original defects in the form of cracks and voids, which impair the load carrying capacity of the structure. If the material is assumed to fail owing to the presence of a defect, it could be reasoned that the stress in the neighbourhood of the defect has reached a critical value. One of the applications that fracture mechanics has in engineering design is to determine the critical load of the structure, based on the size and location of the defect. Therefore, an understanding of the nature of the crack in terms of its geometry and stability is the key to understanding the mechanism of failure. Fracture mechanics as applied to engineering is used to determine the capacity of a structure with an inherent defect to bear a load. Thus with the new design philosophy the following questions arise:

1) What is the maximum crack size that a material can sustain safely?

2) What is the strength of the structure as a function of crack size?

3) How does the crack size relate to the applied loads?

4) What is the critical load required to extend a crack of known size, and is the crack extension stable or unstable?

5) How does the crack size increase as a function of time? [Gdoutos 1990]

To answer the above questions a parameter called the crack driving force is defined which is a function of crack size, geometry, material properties, and loading conditions. The critical value of the crack driving force is called the fracture toughness, which expresses the ability of the material to resist fracture in the presence of a given crack. Inglis (1913) showed that local stresses around an elliptical hole would be several times that of the applied stress. His investigation gave the first real clue to the mechanics of failure, for the reason that an infinitesimally narrow elliptical hole in the limit, could be considered to represent a *crack*. Griffith (1920) was the first to investigate the nature of cracking in his work involving the fracture of glass. He considered an isolated crack in a solid subjected to an applied stress and formulated a basis for its extension in terms of the energy theorems of classical mechanics and thermodynamics. He explained the size effect - the thinner a specimen of a glass rod is, the greater is its strength - and propounded a new theory of fracture of solids. He also discovered that the fracture strength is inversely proportional to the square root of the crack size, in brittle fracture.

However it was not until almost after the end of the second world war that his theory received attention. It was Irwin (1958) who used the singular stress field, derived earlier by Williams (1952) using the eigenfunction expansion method, to introduce the concept of the stress intensity factor. What is characteristic of the stress distribution at the base of a stationary, part through crack, is the fact that a square root singularity exists at the crack front where the stress gradient is large [Williams 1957]. The fracture mechanics method uses the stress intensity factor to describe the elastic stress field at the crack front. A fundamental principle of linear-elastic fracture mechanics is that the stress field ahead of the crack is characterised by a single parameter K. Hence K acts as a scaling factor for the crack tip stress field. This factor is a function of the applied stress field, crack length and geometry. The stresses and displacements ahead of the crack tip shown in Figure 2.2, derived by Irwin (1958), are given by:

$$\begin{aligned} \sigma_{ij} &= K\,(2\pi r)^{-\frac{1}{2}}\, f_{ij}(\theta) \\ u_i &= \left[\frac{K}{2E}\right]\left[\frac{r}{2\pi}\right]^{\frac{1}{2}} f_i(\theta) \end{aligned} \tag{2.4}$$

where $f_{ij}(\theta)$ and $f_i(\theta)$ are functions of θ in the expressions for stress and displacement respectively. K is the stress intensity factor for the corresponding mode of deformation. Once the stress intensity factors have been determined, a fatigue crack propagation law, such as Paris' equation, is used to obtain the number of cycles before failure (fatigue life) in the region of stable crack growth.

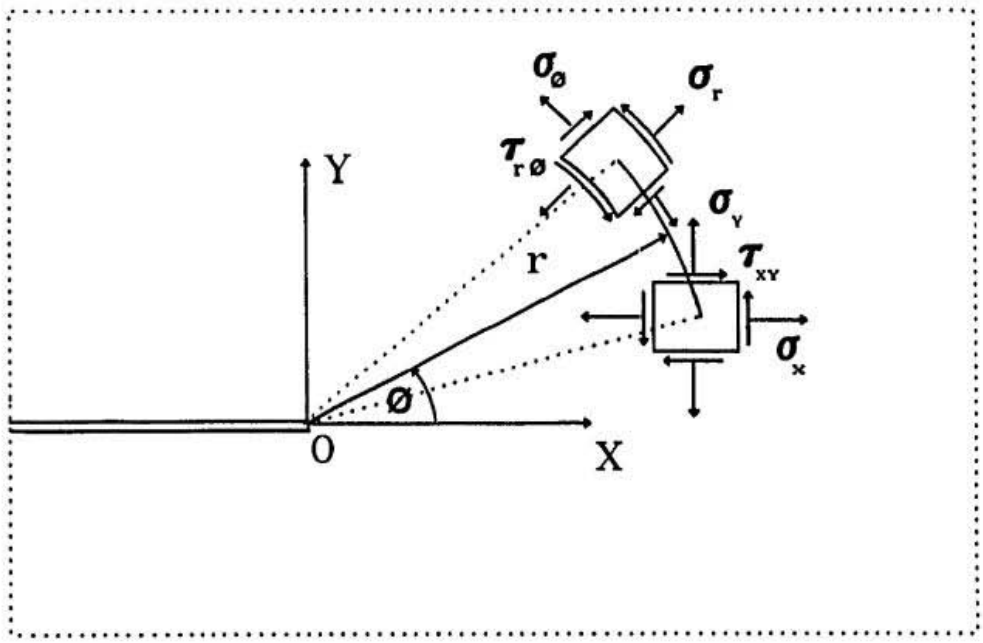

Fig. 2.2 Rectangular and polar stress components around a crack tip: plane stress and plane strain states

A clearer understanding of fatigue could be had, if the fatigue life is resolved into three characteristic stages of initiation, propagation, and fracture. Initiation is analyzed at the microscopic level while propagation is analyzed at the continuum level. The total fatigue life is given by:

$N_T = N_i + N_p$

N_i = Cycles during crack initiation

N_p = Cycles during crack propagation

Crack initiation cannot be defined precisely. For small notched components like welded joints, it is usually assumed that N_i is the number of cycles within which a crack of an initial size - usually of the order of tenths of a mm - grows. Fatigue

resistance of test specimens subjected to stress reversals up to about 10^3 cycles is known as low cycle fatigue, during which time it could be assumed that crack initiation takes place. The fatigue crack initiation life N_i of a notched specimen can be evaluated by any one of the four empirical equations given in eqn. (2.5). Dowling (1979) and Lawrence (1980) have shown that the local stress-strain approach can be used to estimate the crack initiation life while the fracture mechanics approach can be used to estimate the propagation life. Engesvik (1982) has suggested that the size of the region of plasticity is of the same order as a typical grain size, i.e., about 0.01 mm and that the initial crack size should be much greater than the plastic zone size.

Stress Method

$$\sigma_a = \left(\sigma'_f - \sigma_0 \right) \left(2N_i \right)^b \qquad \text{Morrow (1968)}$$

Strain Method

$$\xi_a = \frac{\left(\sigma'_f - \sigma_0 \right)}{E} \left(2N_i \right)^b + \xi'_f \left(2N_i \right)^c \qquad \text{Socie et. al. (1978)}$$

Stress - Strain Method

$$\sigma_a \, \xi_a = \frac{\left(\sigma'_f - \sigma_0 \right)^2}{E} \left(2N_i \right)^{2b} + \left(\sigma'_f - \sigma_0 \right) \xi'_f \left(2N_i \right)^{(b+c)} \qquad (2.5)$$

Manson - Coffin relationship for low cycle fatigue

$$\frac{\Delta\xi}{2} = \frac{\sigma'_f}{E} \left(2N_i \right)^b + \xi'_f \left(2N_i \right)^c$$

where σ'_f = fatigue strength coefficient; ξ'_f = fatigue ductility coefficient; σ_a = notch stress amplitude; ξ_a = notch strain amplitude; σ_0 = notch mean stress; $\Delta\xi = \Delta\xi_e + \Delta\xi_p$, the subscripts e and p refer to the elastic and plastic ranges in the stress-strain hysteresis curves; b = fatigue strength exponent; c = fatigue ductility exponent.

An accurate prediction of the fatigue crack propagation life is important to determining fatigue life. From a design point of view, the question may be stated as follows; determine the number of cycles that an engineering component can withstand before a crack can grow from an initial crack size a_0 to a maximum permissible size a_c. Fatigue crack propagation data are obtained from the crack specimens subjected to fluctuating loads and the change in crack length is recorded as a function of loading cycle.

One of the earlier mathematical models of fatigue crack propagation was proposed by Head (1953). He considered an infinite plate with the central crack of length 'a' subjected to a sinusoidally applied stress $\pm\sigma$. Modelling the elements ahead of the crack tip as rigid-plastic work hardening tensile bars and the remaining elements as elastic bars, he arrived at the relation;

$$\frac{da}{dN} = C_1 \sigma^3 a^{\frac{3}{2}} \tag{2.6}$$

where 'a' is the crack length, N is the number of cycles, the applied stress is σ, and C_1 is a constant. This can also be written in terms of the stress intensity factor by

$$\frac{da}{dN} = C K_I^3 \tag{2.7}$$

The fatigue crack propagation law, proposed by Paris and Erdogan (1963) is a generalised equation of the one above derived by Head and is a widely used crack propagation law, eqn. (2.8).

$$\frac{da}{dN} = C(\Delta K)^m \tag{2.8}$$

where $\Delta K = K_{max} - K_{min}$, with K_{max} and K_{min} refer to the maximum and minimum values of the stress intensity factors in the load cycle. The constants C and m are determined experimentally from a plot of log (ΔK) vs. log (da/dN). The value of m is usually in the range $2.5 \leq m \leq 4.5$ for welded steel and is usually assumed to be equal to three, by reason of which it is called the third power law while C is assumed to be a material constant. Paris' equation does not however account for the crack growth behaviour at low and high levels of ΔK. As K_{max} approaches the critical level K_c, an increase in crack growth is observed. Forman et. al. (1967) proposed the following:

$$\frac{da}{dN} = \frac{C(\Delta K)^m}{(1-R)K_c - \Delta K}; \quad R = \frac{K_{max}}{K_{min}} \tag{2.9}$$

where C and m are material constants and K_c is the critical stress intensity factor. For low values of ΔK Donahue et. al. (1972) have proposed the following:

$$\frac{da}{dN} = C\left(\Delta K - \Delta K_{th}\right)^m \tag{2.10}$$

where ΔK_{th} denotes the threshold value of ΔK. Klesnil and Lucas (1973) showed that the crack growth rate given below is valid in the propagation and fracture regions and that ΔK_{th} is given by:

$$\frac{da}{dN} = C\left(\Delta K^m - \Delta K_{th}^m\right); \quad \Delta K_{th} = (1-R)^{\gamma}\Delta K_{th}(0) \tag{2.11}$$

where $\Delta K_{th}(0)$ is the threshold value at R=0, and γ is a material parameter. Erdogan and Ratwani (1970), Austen and Walker (1977), and Schütz (1981) proposed

generalized crack propagation laws, which are applicable in all three regions of crack growth. Given below is the equation obtained by Erdogan and Ratwani (1970):

$$\frac{da}{dN} = \frac{C(1+\beta)^m(\Delta K - \Delta K_{th})}{K_c - (1+\beta)\Delta K}; \quad \beta = \frac{K_{max} + K_{min}}{K_{max} - K_{min}} \qquad (2.12)$$

where C and m are empirical constants. Dowling and Begley (1976) and Dowling (1977) suggested an equation of the form:

$$\frac{da}{dN} = C(\Delta J)^m \qquad (2.13)$$

to incorporate the J-integral concept to elastic-plastic crack propagation. However the J-integral cannot be applied to elastic-plastic problems if unloading occurs. ΔJ is the variation of J owing to a change in the effective crack length due to plasticity.

Broek (1974) concluded that many of the above empirical formulae are found to be reasonably accurate in a limited region or for a limited set of data. Thus no particular expression for crack growth rate will have significant advantages over the others. Although the fracture mechanics approach has much potential, the method has not been developed to a degree that would render it a standard failure criterion. The fracture mechanics approach is often used in residual life calculations and is based on a crack growing from an initial size to a critical size. This method does not use a fixed failure criterion.

2.2.1 Modes of Crack Extension.

Consider a crack extending along the *XZ* plane through the thickness (Fig. 2.2). Let the crack front be parallel to the Z-axis with the origin of the system of axes at the midpoint of the crack front. Irwin (1958) drew attention to the fact that there are three independent kinematic movements of the upper and lower crack surfaces. The relevance of the crack extension modes is that an arbitrary crack extension could be resolved into one or a combination of modes in the analysis. These modes are illustrated in Fig. 2.3.

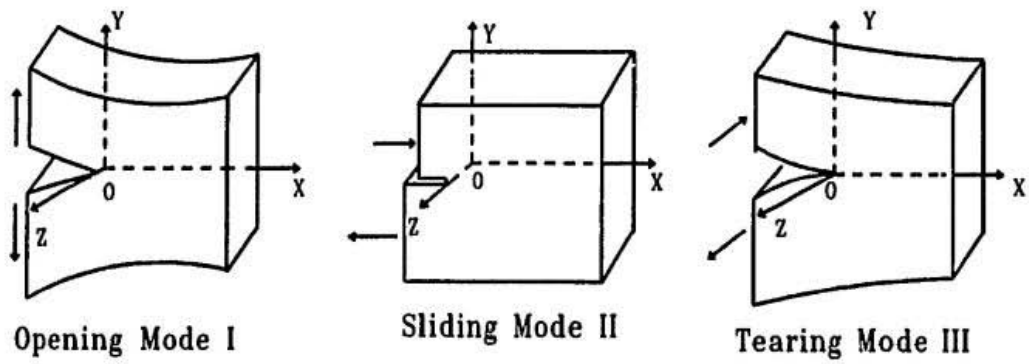

Fig 2.3 The three basic modes of crack extension.

The three modes are defined as follows:

1) Opening Mode I. The crack surfaces separate symmetrically with respect to the planes XY and XZ.

2) Sliding Mode II. The crack surfaces slide relative to each other while maintaining symmetry and skew-symmetry with respect to the planes XY and XZ, respectively.

3) Tearing Mode III. The crack surfaces slide relative to each other while being skew-symmetric with respect to planes XY and XZ.

2.3 Developments in The Finite Element Method

The finite element method is used widely, to solve two-dimensional and three-dimensional boundary value problems. Solutions could be derived using one of the two types of elements which are commonly used for the purpose, viz., (i) conventional and (ii) singular elements. The disadvantages in using the conventional elements is that a very large number of elements is needed to model the region close to the crack tip. On the other hand, the singular elements have the requisite square root singularity embodied in the formulation and hence a smaller number of elements could be used to model the crack tip. Henshell and Shaw (1975) and Barsoum (1976) proposed that the sought after square root singularity at the crack tip could be achieved by displacing the mid-side node in an eight noded quadrilateral isoparametric element to a distance of a quarter length of the side of the corner node where the singularity is needed; this is achieved by requiring that the Jacobian [J] be singular at the crack tip, or that the determinant of **J** vanish at the crack tip. It has also been shown that the element contains the rigid body motion modes, constant strain modes, satisfies the necessary conditions for convergence and passes the patch test [Irons and Razzaque 1972], which the other special crack tip elements lack. Barsoum (1977) proposed collapsing one side of an isoparametric element to form a triangular element with quarter point nodes. He also showed that triangular elements possessed the same singularity in the interior as

well as on the boundary. These elements could have either $1/\sqrt{r}$ or $1/r$ singularity while rectangular elements have a $1/\sqrt{r}$ singularity only on the boundary. The alternating method developed by Shah and Kobayashi (1972), and Smith (1972) uses two analytical elasticity solutions for infinite and semi-infinite solids. The first solution is for an elliptical crack in an infinite solid. The second solution is for an un-cracked semi-infinite body subjected to uniform normal and shear stresses. Pian and Moriya (1977) proposed the hybrid singular elements; they are the stress-hybrid and displacement-hybrid elements. The advantage in using these elements is that the stress intensity factors, K_I, K_{II} and K_{III} are obtained as part of the solution. In these elements, the stress singularities are represented by K_I, K_{II} and K_{III}, and the near field two-dimensional stress solutions at the crack front.

2.3.1 Extraction of stress intensity factors

If the stress intensity factors are included in the finite element formulation, they are evaluated once the problem is solved. The stress intensity factors are obtained directly from the solution if the following elements are used: the enriched element of Benzley (1974), and Hilton (1977); and the stress hybrid element of Tong and Atluri (1977), and Atluri et. al. (1978). However, if any other type of element is used, the stress intensity factors have to be derived from the finite element solution. Three methods are used for the derivation; they are the crack-opening displacement method, the virtual-crack extension method, and the force method.

2.3.2 Crack-opening displacement method

The crack opening just behind the crack front is compared with the corresponding two-dimensional case to determine the stress intensity factor. The two-dimensional solution assuming plane strain is given below.

$$v = K_I \frac{4 (1 - \nu^2)}{E} \sqrt{\frac{r}{2 \pi}} \qquad (2.14)$$

where v is half of the crack opening displacement at a distance of r from the crack front. Two methods are used in the evaluation. In the first method the crack opening displacement at the node next to the crack front is substituted in the equation above to derive K_I. In the second approach the crack opening displacement values at various locations from the crack front are used to derive the apparent stress intensity factor. Linear regression is used thereafter to determine the value at K_I at r = 0. The conventional finite element method of Miyamoto and Miyoski (1971) and Ando and Yagawa (1977); the quarter point element of Barsoum (1977), and Wu (1984); and the singular element of Tsang (1981) are used in the first method while the singular elements developed by Henshell (1975), Boom and van Fossen (1976), and Blackburn and Hellen (1979) have been used with the second method. The negative feature of the approach is that the state of stress around the crack front of being either plane strain or plane stress has to be presupposed. Such a presupposition yields a factor of (1 - ν^2) in the case of plane strain, by which the stress intensity factors differ. The plane strain assumption is made along the crack front and the plane stress condition is

assumed where the crack front meets the free surface.

2.3.3 Virtual Crack Extension Method

Hellen (1975), McGowan and Raymund (1979), Blackburn and Hellen (1979), and Hall et. al. (1979) have used this method extensively. The stress energy release rate G is computed and the stress intensity factor is derived from it. The strain energy release rate is given by $-\frac{\partial U}{\partial c}$ where U is the strain energy of the structure and c is half the crack length. The stress intensity factor K_I can be calculated from:

$$G = \frac{K_I^2}{E'} \tag{2.15}$$

where E' is a material constant. Parks (1974), and Hellen (1975) extended the method to analyze three-dimensional problems.

2.3.4 Force Method

The forces ahead of the crack front and normal to the crack plane are used to evaluate the stress intensity factors. In the two-dimensional case, the near field stresses ahead of the crack tip are the same for the plane stress and plane strain situations. Therefore, the use of the two-dimensional stress solution ahead of the crack tip would eliminate an assumption of the stress state. Raju and Newman (1977 a-c, 1979 a,b) used the finite element forces ahead of the crack front and normal to the crack plane and compared these results with those obtained by integrating the near field stresses from the two-dimensional solution. The stress intensity factors were evaluated as in

the COD method.

2.4 Line Spring Model

The main idea of the line-spring model is the substitution of a three-dimensional body with a part through surface crack, by a two-dimensional body with a part-through crack. The increase in the compliance of the member is accounted for by the introduction of line-springs, each of which is equivalent to a single edge-cracked plate under plane strain conditions. Fig. 2.4 gives an illustration of the concept [Akimin and Nikishkov, 1989]. The virtue of the line-spring model is in its simplicity. It reduces the three-dimensional problem to one of being a two-dimensional problem. The line-spring model has been proven to reduce the time of computation in comparison with other numerical methods. It has also proven to be useful in studying the effects of plasticity in shell plate structures in a part-through crack problem. The line-spring model for surface flaws was originally proposed by Rice and Levy (1972). This formulation is based on the Poisson-Kirchhoff bending theory for thin plates and shells. Subsequent developments have used the Reissner plate theory to take into account the shear in the transverse direction. However, Parks (1981) pointed out that the discrepancy between the higher order plate theory and the classical theory is not significant if the length of the crack is larger than the thickness of the plate or shell (i.e., if the crack is not a short and deep crack).

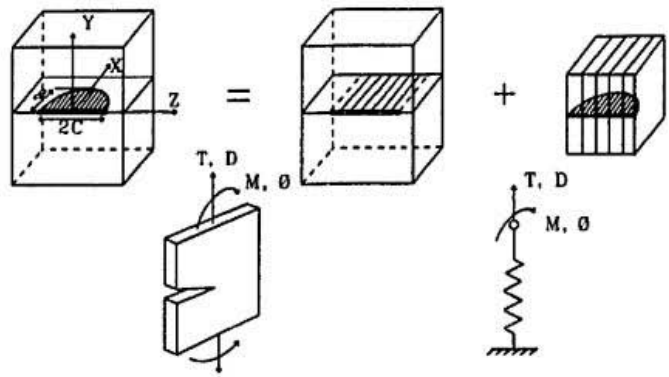

Fig. 2.4 The concept of the line-spring model

Rice and Levi (1972) analyzed a plate, containing a surface crack penetrating through part of the thickness and subjected to tensile stretching and bending, with its compliance coefficients being chosen to match those of an edge crack strip in plane strain. To illustrate the strengths of the line-spring model, the problem described above was solved using the finite element method by German et. al. (1983). With this model, Rice and Levi (1972), Parks et. al. (1981), Delale and Erdogan (1982), and German et. al. (1983) analyzed the surface cracks in plates and cylindrical shells. Parks (1981) used the line-spring model to estimate the J-integral and crack tip opening displacement for some surface cracks in plates and shells. Kumar and German (1985) used it with the J_2 deformation theory of plasticity to obtain a fully plastic crack solution. Earlier Dill and Saff (1978) developed the slice-synthesis model similar to the line-spring model, which was applied to surface cracks and plates.

The limitations of the line-spring model are:

1) That it can be applied to plates and shell structures only.

2) That accuracy suffers when the aspect ratio of the crack is very small. The

aspect ratio is given by a/c, where a is the depth of the crack and c is half the length of the crack which is assumed to be elliptic.

3) That the stress intensity factors are lower if there is a stress concentration near the crack site, as shell models can only describe linear stress distributions through the thickness [Du and Hancock, 1989].

2.5 Applications

2.5.1 Semi-Elliptical surface cracks in a plate

Several investigators have worked on the problem of semi circular cracks (a/c = 1) in plates. With shallow crack depths, i.e., a/T < 0.2, Tracey (1974) used the six noded singular element with the crack opening displacement method; Pian and Moriya (1978) used the stress-hybrid elements; Blackburn and Hellen (1979) used the fifteen noded singular element and the virtual crack extension method while Yagawa and Nishioka (1980) used the superposition method. The solutions obtained by these individuals compared favourably with one another.

Newman and Raju (1979) reviewed the solution of the surface crack problem to cover a broad range of crack growth parameters; ($0.2 \leq a/c \leq 1$) and ($0 \leq a/T \leq 0.8$) where a is the crack depth, c half the crack length and t the cross sectional thickness. For shallow cracks $a/T \leq 0.3$, and near semi-circular cracks $0.6 \leq a/c \leq 1$, the stress intensity factors obtained by: Smith and Alavi (1971), and Shah and Kobayashi (1972) using the alternating method; Raju and Newman (1977 a-c) using the

finite element method; and Newman and Raju (1979 a,b) using the line-spring model, showed good agreement. The results obtained for deeper ($a/T > 0.3$) and semi elliptical $0.2 \leq a/c \leq 0.6$ cracks were less promising. The results showed considerable discrepancies, which Newman believed was the result of improper definition of the boundary conditions.

Parks et.al. (1981) and German et. al. (1983) analyzed surface cracks with $0.2 < a/c < 0.667$ with $0.2 < a/T < 0.8$. Delale and Erdogan (1982) and Dill and Saff (1978) analyzed surface cracks with $a/c = 0.2$ at $a/T = 0.4$ to 0.8 using the line-spring method. The results obtained by both teams were reasonably consistent at the deepest point; nevertheless the disparity between the results seemed to be the greatest at the free surface. In addition, the results for shallow cracks were more consistent than those obtained for deep cracks. The results were most inconsistent when $a/c = 0.7$ and $a/T = 0.2$ (short and deep cracks).

Although there are many ways to evaluate the stress intensity factors of semi elliptical cracks, notably the line-spring method of Rice and Levy (1972) has been extensively applied to tubular joints and flat plates by Kumar, German and Schumacher (1985) because it is computationally efficient. The basic method developed by Rice and Levy for mode I has been extended by Parks (1981) and Desvaux (1985) to include modes II and III also. They also found agreement better than 3% between the line-spring calculation and a full three dimensional solution at the deepest point of the crack

with an aspect ratio a/c of 0.2, in a flat plate.

2.5.2 Line spring and three-dimensional analysis of a tubular joint

Chu (1984) and Burdekin (1985) showed that the local stress concentration affects only the stresses near the surface of the tubes where the stresses deviate from the thin shell theory over about 20% of the plate thickness. Cracks subject to this local stress concentration cannot be modelled effectively by the line-springs unless account is taken of the local stress concentration by using a correction factor. The development of a crack, growing on a curved path under the chord-brace intersection, can be predicted by considering the orientation of a small angled kink on the crack tip which maximizes either K_I or G. The close agreement between experimental and computed data shows that the local stress concentrations, caused by the weldments, which have not been modelled, has no effect on the analysis. Dover et. al. (1991) came up with a simple relation for a wide range of crack shapes, given by the following equation:

$$\frac{a}{c} = 0.167 \left(\frac{a}{T} \right) + 0.05 \qquad \left(\frac{a}{T} \geq 0.2 \right) \tag{2.16}$$

These ratios compare favourably with computed and experimental data.

Huang et. al. (1988) modelled a tubular welded T-joint containing semi-elliptical cracks located at the chord and brace intersection which was analyzed using the line-spring model and the virtual crack extension method. The chord and brace were

modelled with eight noded curved shell elements while the critical region of the chord-brace intersection was modelled using twenty noded isoparametric brick elements. Compatibility between the bricks and shell elements was achieved using transition elements which had eighteen, twelve and fifteen nodes produced by degenerating twenty noded brick elements. The same joint was also modelled using eight noded doubly curved shell elements with the cracks represented by the line-spring model. The mesh was generated using commercial codes and were optimized by the method suggested by Sloane and Randolph (1983) for the frontal solution. The models were subjected to uniform axial force on the brace and the ends of the chord were built in. Three crack geometries were analyzed which consisted of semi elliptical cracks with a maximum depth to thickness ratio a/T of 0.6 and 0.9 and a surface length 2c/T = 4. They concluded that the line-spring concept of Rice and Levy provides a flexible and computationally efficient method of calculating the stress intensity factors of cracks in tubular joints for cracks with depths greater than a/T = 0.2; the computational effort being comparable to determining the hot spot stress concentration by shell analysis. The line-spring, and the three dimensional solutions yielded results that were consistent to within 3.5% at the deepest point and showed good agreement along the whole crack front; shallow cracks showed similar results with a discrepancy of 2.5% at the deepest point.

2.6 Stress Intensity Factor Evaluation

Central to the application of linear elastic fracture mechanics in fatigue analysis

is the determination of the stress intensity factor ranges. Stress intensity factor solutions are now available for a wide range of geometries, e.g., Special Technical Publications by the American Society for Testing and Materials [ASTM Standards 1981]. Unfortunately, the available solutions to evaluate the stress intensity factors prove inadequate where a structure has a complex geometry and loading. Thus there is a need to develop simpler and inexpensive methods, even at the expense of being less accurate than the established methods.

An equivalent stress intensity factor based on the energy release rate is defined as;

$$K_e = \left[K_I^2 + K_{II}^2 + \frac{K_{III}^2}{(1-\nu)} \right]^{\frac{1}{2}} \tag{2.17}$$

for a mixed mode fracture problem, where K_I, K_{II}, and K_{III} are the stress intensity factors for three independent modes and ν is the Poisson's ratio. Rhee et. al. (1991) developed an empirical formula by which the stress intensity factor solutions at the crack front point on a curved tubular surface could be evaluated and is given by:

$$K_e = F(\beta, \gamma, a', c')\, \sigma_N \sqrt{\pi a} \tag{2.18}$$

where $a'=a/T$, $c'=3c/d$, $\tau=t/T$, $\gamma=D/2T$, $\beta=d/D$, a is the crack depth, T is the chordal thickness, c is the crack length, d is the brace diameter, t is the brace thickness, D is the chordal diameter, σ_n is the nominal stress and $F = F_g F_s F_i$. F_g is the joint geometry

factor, F_s is the crack size factor and F_i is the joint and crack coupling factor.

Haswell and Dover (1991) found out that the stress intensity factor solutions for tubular joints are influenced by the degree of bending and crack shape assumptions. Pook et. al. (1992) observed that: (i) mixed mode loading may occur when a crack developed under forces acting along one axis is subjected to a force applied along another axis, and (ii) mixed mode stress intensity factors cannot be determined analytically and that numerical methods could prove costly. Consequently the approximate mixed mode stress intensity factors for part-through cracks in tubular welded joints could be modelled as warped part-through surface cracks for Mode I and approximations for Modes II and III could be based on the exact analytical solutions for an elliptical crack in an infinite body.

The general formula for the stress intensity factor of edge cracks in two dimensions is given in eqn. (2.17). Dijkstra et. al. (1993) show that

$$K = [M_{k,m}\, M_m\, \sigma_m + M_{k,b}\, M_b\, \sigma_b] \sqrt{(\pi a)} \qquad (2.17)$$

where M_k is the stress intensity concentration factor for the influence of the weld geometry, M is a correction factor for a flat strip or plate and indices m and b are for membrane and bending, respectively. More information on how to determine the geometrical correction factors M and M_k can be found in the studies of Dijkstra et. al. (1989), and Van Straalen and Dijkstra (1993). Ritchie and Voermans (1985), and Kristiansen and Fu (1993) analyzed surface cracks in welded tubular joints. The values

obtained along the crack front showed good agreement between estimated and computed values except at the free surface. The latter concluded that: (i) the stress intensity factor ratio $\alpha_k = \frac{k_I\,(\text{free surface point})}{k_I\,(\text{The deepest point})}$ is affected by various factors in particular by the weld notch stress concentration; (ii) in tubular joints an increase in the stress intensity factor occurs in a limited free surface region, which they attributed to the curved crack configuration and varying stress distribution along the joint intersection; and (iii) the displacement approach could give reasonable approximations if it is used with a detailed three dimensional mesh. Nwosu (1993) verified that with suitable modifications and the correct contact algorithm, the use of line-spring elements was found suitable for evaluating the stress intensity factors in tubular welded joints. Bowness and Lee (1993) concluded that a cracked T-joint model, in which chord saddle cracks were simulated using line-spring elements was successfully validated against existing experimental and three dimensional results.

2.7 Fatigue Life of Tubular Welded Joints

The phenomenon of fatigue crack initiation which is studied at the microscopic level is a very complicated problem and a few quantitative theories have been proposed for its study. Fatigue cracks generally occur at localized high stress concentration regions where the stress exceeds the yield stress of the material. Since the loading in the brace is an axial or bending load, the weld toe crack propagation will be predominantly the opening mode. Dover and Dharmavasan (1982) showed that the

cracks present in tubular joints grow steadily through the wall thickness at a fairly constant rate. Wylde and McDonald (1981) showed that cracks of size 1 to 3 mm were present at less than 10% of the total life of a welded tubular joint. de Back and Vaessen (1981) showed that initiation life is about 30% of the crack-through life for a tubular T-joint. For a case of axial loading Munaswamy et. al. (1987) showed that the crack initiation life was about 34.6% of the total life in air at 250 MPa (hot spot nominal stress) and 46.6% in simulated sea water at 160 MPa. Yagi et. al. (1991) investigated the effect of thickness in welded steel joints and observed that the thickness had the largest effect on crack initiation, whilst having little effect on crack propagation. Bell & Vosikovsky (1992) pointed out that many cracks initiate along the weld toe and grow into one another to form fewer and larger cracks. Hence the actual shape of a crack is governed more by coalescence rather than by crack growth of a single elliptical crack. It was also found that coalescent life was a significant percentage of the propagation life. To estimate the contribution of crack coalescence in the propagation life, an empirical crack shape development function was developed and given by:

$$\frac{a}{c} = e^{-ka} \tag{2.18}$$

where k is a function of the stress level and weld toe geometry. Nwosu (1993) concluded that the ratios of crack initiation life to total life range from 13-26% for axially un-stiffened tubulars, from 34-55% for in-plane bending loads, and from 12-24% for out-of-plane bending loads, and that the local strain approach could be used

successfully to predict the fatigue crack initiation life of tubular welded joints. Skorupa and Skorupa (1993) studied the fatigue crack initiation period of welds in structural steels failing at the weld toe. For their study, they analyzed a cruciform welded joint in mild steel subjected to axial stresses. They concluded that: (i) in the presence of a high positive notch mean stress, the fatigue crack initiation life N_i estimates based on low cycle fatigue provided inconsistent values; and (ii) only the two stage approach, which includes initiation and propagation enables satisfactory prediction of the total life in both, sound and under-cut welds. Pang (1993) modelled and analyzed the behaviour of semi-elliptical crack coalescence and growth. A comparison between the computational result and testing showed that at low stresses there was good agreement, while the same could not be said for higher stresses, although the computed life was conservative. Tos et. al. (1993) used two models of a welded joint with multiple semi-elliptical cracks to model the crack shape development; they observed that: (i) while the multiple crack model provides a better simulation of crack shape development and fatigue life, both models were found to under-predict the fatigue life when the total stress range was used in the integration of Paris' equation; and (ii) differences in crack shape development are largely responsible for the differences in the predicted lives between the forcing function simulations and the multiple crack simulations. Bucak et. al. (1994) showed that the hot spot stresses affected the development and propagation of cracks in welded hollow joints. They considered several forms of cracks to analyze the crack propagation pattern changes and proposed a modified cumulative damage rule.

2.8 Summary

The literature that has been reviewed relates to the developments in the application of the finite element method and the application of linear elastic fracture mechanics for assessing the fatigue life of a cracking tubular T-joint. It has also been observed that since the line-spring elements do not model correctly, the nonlinearity of surface stresses around the crack or singularity region, the results obtained by them are not good around surface penetrating zones. Also for short and deep cracks the line-spring elements do not give good results. The subsequent chapters describe the application of the line-spring model to a tubular T-joint subjected to an axial load. The cracked structure has been modelled using line-spring elements.

Chapter 3

Theoretical Background

3 General

The analysis of tubular joints would require the methods used in the analysis of shell structures. A shell is the "...materialisation of a curved surface" [Flügge (1960)], in which the normal stress through the thickness is considerably smaller than the in-plane stresses and thus is neglected in the analysis. While analytical solutions available for shell structures are limited in their application to the many and varied joint design situations, the finite element method has evolved to be a proven numerical technique. The possible type of elements that could be used in the finite element analysis could be broadly categorized as:

1) Thin shell elements (Kirchhoff assumptions);

2) Thin/thick shell elements (Reissner-Mindlin theory);

3) Three dimensional elements;

4) Modified or degenerated three dimensional elements;

The constraint imposed in the Kirchhoff theory is that the normal to the shell's reference surface remains normal throughout the deformation phase. In the Reissner-Mindlin Theory, shear flexibility is assumed, which is to mean that the normals at the

top and bottom surfaces may not lie in a straight line during deformation. Three dimensional elements give improved modelling at the tubular joint intersections and have been used to model the joint along with the regular thin shell elements. In the modified three dimensional category, the most noteworthy formulation is the degenerated isoparametric element, in which the three dimensional stress and strain conditions are degenerated to shell behaviour. This was originally introduced by Ahmad et.al. (1970). There are many kinds of degenerated elements, which are used in the linear and nonlinear analyses of thin or thick shells [Hinton and Owen, 1984]. Degenerated elements need only C^0 continuity of displacements across the inter-element boundaries compared with other elements based on shell theory. Hence it is advantageous to use such elements in estimating the stress intensity factors of tubular joints. The eight noded degenerated serendipity shell element, shown in Fig. 3.1, is one such element that has been used by many in the analysis of tubular joints; hence that element is used in this investigation. The degenerated element was improved considerably by the reduced integration method, with the intention of avoiding the incidence of "self locking" [Wu and Abel, 1991]. The assumptions in the formulation are:

1) The normals to the mid-surface remain normal throughout the deformation stage.
2) The strain energy corresponding to the stresses perpendicular to the mid surface is disregarded, i.e., they are constrained to be zero.

Five degrees of freedom are considered at each node, consisting of three translations and two rotations. The two rotational degrees of freedom correspond to

rotations about the two surface axes.

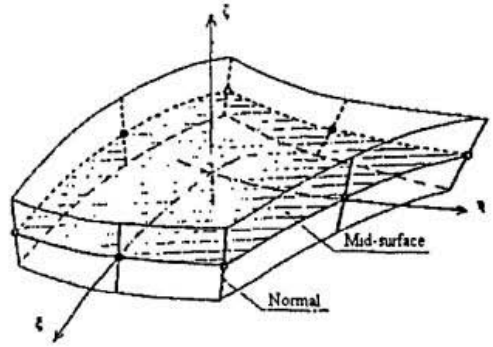

Fig. 3.1 The degenerated isoparametric element, [Hinton and Owen, 1984]

3.1 Coordinate Systems

In defining the geometry of the element, four coordinate systems are employed; they are,

1) Global coordinates

2) Curvilinear coordinates

3) Nodal coordinates

4) Local coordinates

Global coordinate system

The global coordinate system (x, y, z) is a cartesian orthogonal system and is located at a conveniently chosen point.

Curvilinear coordinate system.

The curvilinear coordinate system is a cartesian system, in which ξ, η and ζ are

a set of orthogonal axes. ξ, η are in the middle plane, while ζ lies in the thickness direction. The element is bounded by surfaces given by equations $\xi \pm 1 = 0$; $\eta \pm 1 = 0$; $\zeta \pm 1 = 0$. Fig. 3.2 shows a typical element and its disposition in relation to the axes.

Nodal coordinate system

The origin of the nodal coordinate system is located at the i^{th} node on the mid-surface and is a right-handed system of cartesian coordinates. Such an arrangement is shown in Fig. 3.3. As an infinity of vector directions normal to a given direction can be generated, one particular scheme has to be decided upon. Schemes other than the described below are quite possible. A vector $\mathbf{V}_{1i}$ is derived by taking the vector cross product between the unit vector along the global x axis direction and $\mathbf{V}_{3i}$, i.e., $\mathbf{V}_{1i} = \mathbf{i} \otimes \mathbf{V}_{3i}$; $\mathbf{V}_{3i} = \{x_p\}_{top} - \{x_p\}_{bottom}$, where p=1,2,3 is a tensor index used instead of the conventional *i*. $\mathbf{V}_{2i}$ is constructed so that $\mathbf{V}_{1i}$, $\mathbf{V}_{2i}$, $\mathbf{V}_{3i}$ form a right-handed cartesian coordinate system. If $\mathbf{i} \otimes \mathbf{V}_{3i} = 0$; then $v_{1i} = \mathbf{j} \otimes \mathbf{V}_{3i}$, **i**, and **j** are unit vectors in the global x and y directions; *i* denotes the *ith* node.

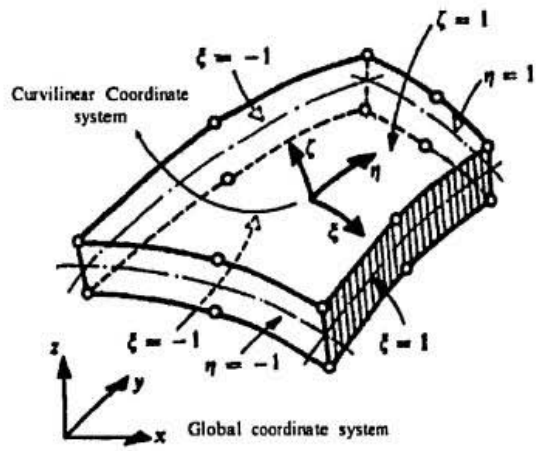

Fi.g 3.2 The curvilinear coordinate system of a shell element and its disposition to the global axes [Zienkiewicz 1977]

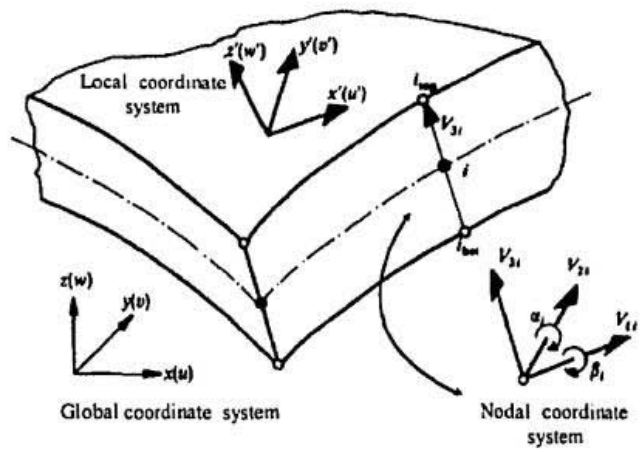

Fig. 3.3 The coordinate systems and associated displacements for a degenerated isoparametric element [Zienkiewicz 1977]

Local coordinate system

This is a cartesian system of coordinates defined at the sampling points wherein stresses and strains are to be calculated and is shown in Fig 3.3. The axis perpendicular to the surface termed z′, is taken perpendicular to the surface ζ=constant; the other two local axes x′ and y′ are determined to complete an orthogonal triad. Such a coordinate system is used to calculate the stresses and strains at the sampling point.

3.2 Element geometry

With reference to Fig. 3.2, the external faces of the element are curved, while the sections across the thickness are straight lines. The curvilinear coordinate ζ is approximately normal to the mid-surface, since it may not lie in the thickness direction. The global coordinates of the top and bottom points that correspond to a given node on the mid-plane surface are used to define the element geometry. In the isoparametric

formulation, the coordinates of an arbitrary point are given in terms of the nodal coordinates and shape functions. A relationship between the global and curvilinear systems for any point within the element is given by:

$$\{ x_p \} = \sum_{i=1}^{8} N_i(\xi,\eta) \frac{(1+\zeta)}{2} \{ x_p \}_{top} + \sum_{i=1}^{8} N_i(\xi,\eta) \frac{(1-\zeta)}{2} \{ x_p \}_{bottom} \quad (3.2)$$

where N_i is a shape function that takes the value of unity at node i which is a node on the edge of the mid-surface as shown in Fig. 3.3. The number eight denotes the number of shape functions, p is a tensor index, used instead of i. Alternately the above equation can be written in terms of the mid-surface nodal coordinates and the vector connecting the top and bottom points, which gives the directional thickness, as shown in eqn. 3.3.

$$\{ x_p \} = \sum_{i=1}^{8} N_i(\xi,\eta) \{ x_p \}_{midpoint} + \sum_{i=1}^{8} N_i(\xi,\eta) \frac{\zeta}{2} V_{3i} \quad (3.3)$$

$$V_{3i} = \{ x_p \}_{top} - \{ x_p \}_{bottom} \text{ with } p = 1, 2, 3,$$

3.2.1 Displacement field

The assumption that the strains in a direction normal to the mid-surface are negligible, suggests that the displacement of an arbitrary point could be defined by the translation of its associated mid-point, and the rotation of V_{3i} vector, as indicated in Eqn.(3.1). α_i, and β_i correspond to the rotational degrees of freedom about the mid-surface axes. The element displacement field could then be given by:

$$\{ u_p \} = \sum_{i=1}^{8} N_i(\xi,\eta) \{ u_p \}_{midpoint} + \sum_{i=1}^{8} N_i(\xi,\eta) \frac{h_i}{2} [v_{1i}, -v_{2i}] \begin{Bmatrix} \alpha_i \\ \beta_i \end{Bmatrix} \quad (3.4)$$

where $\mathbf{v}_{1i}$, $\mathbf{v}_{2i}$ are the column unit vectors, h_i is the shell thickness at node i and α_i, and β_i are the scalar rotational quantities as shown in Fig. 3.3, p=1,2,3 is used as before.

3.2.2 Stress-strain formulations

The stresses corresponding to the strains are defined by matrix σ' and are related by the elasticity matrix $\mathbf{D}'$, ϵ_0' and σ_0' represent initial strain and stress states. The matrix $\mathbf{D}'$ includes elastic components for an isotropic material; it could be modified to include anisotropic properties as well.

$$\sigma' = \begin{Bmatrix} \sigma_{x'} \\ \sigma_{y'} \\ \tau_{x'y'} \\ \tau_{x'z'} \\ \tau_{y'z'} \end{Bmatrix} = \sigma' = \mathbf{D}'\left(\varepsilon' - \varepsilon_0'\right) + \sigma_0' \tag{3.5}$$

$$\epsilon' = \begin{Bmatrix} \epsilon_{x'} \\ \epsilon_{y'} \\ \gamma_{x'y'} \\ \gamma_{x'z'} \\ \gamma_{y'z'} \end{Bmatrix} = \begin{Bmatrix} u'_{1,1} \\ u'_{2,2} \\ u'_{1,2}+u'_{2,1} \\ u'_{1,3}+u'_{3,1} \\ u'_{2,3}+u'_{3,2} \end{Bmatrix} \tag{3.6}$$

where $\mathbf{u}'$, ϵ' are the displacements and strains expressed in the local coordinate system and $\epsilon'_{33}=0$, since the stresses are negligible in that direction.

$$\mathbf{D}' = \frac{E}{(1-\nu^2)} \begin{bmatrix} 1 & \nu & 0 & 0 & 0 \\ 0 & 1 & 0 & 0 & 0 \\ 0 & 0 & \frac{1-\nu}{2} & 0 & 0 \\ 0 & 0 & 0 & \frac{1-\nu}{2k} & 0 \\ 0 & 0 & 0 & 0 & \frac{1-\nu}{2k} \end{bmatrix} \tag{3.7}$$

E and ν are the Young's modulus and Poisson's ratio, respectively. The factor k is included to improve the shear deformation approximation, which is seen to be somewhat linear, when in fact for homogeneous cross-sections, the shear stress distribution is known to be parabolic.

3.2.3 Element properties and transformations

Matrices that involve element properties consist of a volume integral which in its general form is given by $\int_{V_e} S\,dx\,dy\,dz$. The matrix **S** is a function of the coordinates. The stiffness matrix, for example, is given by $\mathbf{S}(\xi, \eta, \zeta)=\mathbf{B}^T\mathbf{D}\mathbf{B}$ where **B** is the strain shape function matrix, and **D** is the elasticity matrix. To determine the stresses and strains in terms of the local coordinates, two transformations are necessary.

1) Curvilinear to the global system

2) Global to the local system

The first transformation for the displacement is given by:

$$[\![\, \mathbf{U}_{pj,p} \,]\!] = [\![\, \mathbf{J} \,]\!]^{-1} [\![\, \mathbf{U}_{c_{pj},p} \,]\!] \tag{3.8}$$

This equation relates the displacements $\mathbf{U}_{pj}$ given in terms of the global coordinates to

the displacements $\mathbf{U}_{cpj}$ given in terms of the curvilinear coordinates. The components of the matrices $\mathbf{U}_{pj}$ and $\mathbf{U}_{cpj}$ are the components of the displacement vectors expressed as row vectors, given in terms of the two coordinate systems. $[\![\mathbf{J}]\!] = [\![\mathbf{X}_{pj,p}]\!]$, where $\mathbf{J}$ is the Jacobian and $\mathbf{X}_{pj}$ are the components of a matrix containing the position vector of an arbitrary point within the element as row vectors, being functions of (ξ, η, ζ). The derivatives of the displacement components in the global direction are now transformed to functions of the local coordinates by the transformation:

$$[\![\mathbf{U}'_{pj,p}]\!] = [\![\theta]\!]^{\mathrm{T}} [\![\mathbf{U}_{pj,p}]\!] [\![\theta]\!] \tag{3.9}$$

where $\mathbf{U}'$ and $\mathbf{U}$ are the components of the displacement in the local and global coordinate systems, respectively. The matrix θ is formed by the unit vectors along the directions of the local axes x', y', z', i.e., $\theta = [\![\mathbf{v}'_1, \mathbf{v}'_2, \mathbf{v}'_3]\!]$. The strains are derived from the displacements by the relationship:

$$\epsilon' = \mathbf{B}' \begin{Bmatrix} \mathbf{a}_i^e \\ . \\ \mathbf{a}_n^e \end{Bmatrix}; \qquad \mathbf{a}_i^e = \begin{Bmatrix} u_i \\ v_i \\ w_i \\ \alpha_i \\ \beta_i \end{Bmatrix} \tag{3.10}$$

where i takes the values from *1* to *8*, *8* being equal to the number of nodes; $\mathbf{a}_i^e$ denotes the i^{th} node of an element e [Zienkiewicz 1977].

3.3 Crack initiation

Fatigue initiation is a process of cumulative plastic strain, which is associated with the movement of dislocations that takes place more at the surface than in the bulk of the material. Hence, fatigue initiation is a surface phenomenon although exceptions have been observed, in which case initiation takes place within the material, as in e.g. carburized, case hardened steels. Fig. 3.4 shows such a formation as a result of cyclic stress. Fig. 3.5 shows the stress-strain curve for such a cyclic loading. The total strain has been shown in terms of the elastic and plastic components, of which $\Delta\epsilon_p$ quantifies the permanent deformation [Almar-Næss 1985].

Dowling (1979) proposed a method to estimate the total fatigue life of a notched component. This method combined the local strain approach to predict crack initiation life and a fracture mechanics approach to predict the crack propagation life [Bannantine et. al. 1990]. Crack initiation behaviour is not amenable to the laws of fracture mechanics; hence its life cannot be evaluated by such means. Dowling proposed that when the length of the crack is smaller than the extent of the notch stress field, the strain-life approach could be used to determine the crack initiation life or early growth from a notch. Several factors affect the strain-life such as heat treatment of metals, mean stress effects etc. [Bannantine et. al. 1990]. It has been observed that the crack initiation life becomes significant in the total life of the joint only in the event of small wall thickness, post weld improvements etc. The Manson - Coffin's equation, given below in eqn. (3.11), will be used to determine the initiation life.

$$\frac{\Delta\epsilon}{2} = \frac{\sigma_f'}{E}(2N_f)^b + \epsilon_f'(2N_f)^c \qquad (3.11)$$

The four coefficients required for this analysis, viz., σ'_f , ϵ'_f, b, and c are coefficients whose values will be determined from the results obtained by (Iida 1987) for tubular joints whose chord thicknesses are in the range 0 - 10 mm. σ'_f is the fatigue strength coefficient, b is the fatigue strength exponent, c is the fatigue ductility component, ϵ'_f is the fatigue ductility coefficient, $2N_f$ is the reversals to failure or the initiation life, $\Delta\epsilon$ is the total strain amplitude, and E is the modulus of elasticity.

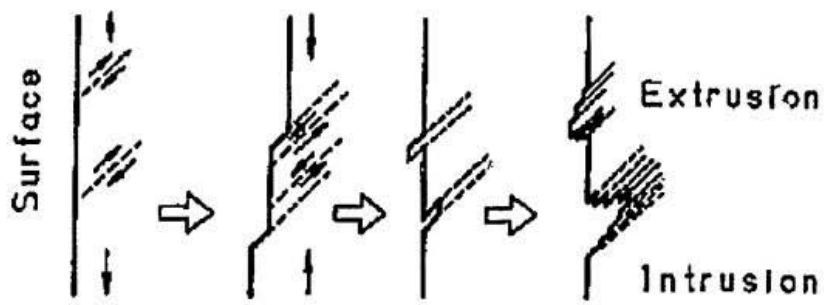

Fig. 3.4 The development of permanent slip bands, caused by plastic flow [Almar-Næss 1985]

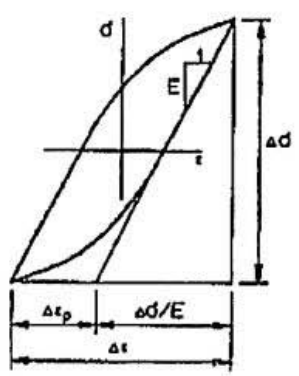

Fig. 3.5 Cyclic stress-strain response [Almar-Næss 1985]

3.3.1 Fatigue Crack Growth Formulation

Fracture mechanics is the discipline concerned with the study of cracks and their behaviour. Under the assumptions of linear elasticity valid for fatigue crack growth problems, the stress intensity factor characterizes the crack tip behaviour. It has been shown that the energy available for fracture or the crack driving force is directly proportional to the square of the stress intensity factor. It may be expected therefore that under fatigue loads, the fatigue crack growth rate will be governed by the variation in the stress intensity factor ΔK during the load cycle. The application of fracture mechanics approach to crack propagation life evaluation requires ascertaining of the stress intensity factors at defects. In tubular T-joints, the most likely area for the presence of defects would be the hot spot zone of the weld toe region. Before the stress intensity factor at a defect could be evaluated, the following have to be known:

1) Crack position
2) Interaction of adjacent cracks
3) Crack profile
4) Residual stresses

Even though multi-nucleation sites are observed during the crack initiation life of a fatiguing structure, only one crack becomes a dominant crack (with an approximately elliptic profile) during the coalescence of these multi-nucleating crack sites; hence only a single crack will be considered in the computation of the crack propagation life of the T-joint. The single crack location or position will vary depending

on the type of applied load/loads acting on the tubular joint; the tendency to crack will mainly depend on the magnitude of the stresses experienced around the maximum stress/strain concentration region of the weld toe, known as the hot-spot, (this region will be determined during the stress analysis phase of the computation). The residual stresses present in the hot-spot region of the weld toe will generally be compressive on the surface of the hot spot region, due to the differential cooling process; hence it will not have any significant influence on the fatigue life of the tubular joint. The factors considered in this study do not take into account the environment and its effects, which in the case of marine environment, could be significant as well as unpredictable.

3.3.2 Line spring model for the evaluation of stress intensity factors

The line spring element has been used to model a crack at a cracked site. This model has proven to be a relatively simple and efficient one for determining stress intensity factors. Rice and Levi (1972) introduced the model by which a surface flawed plate, exposed to far field tension and bending, was analyzed within the context of the two dimensional generalized plane strain and plate bending theory. The part through cracked section is represented as an assemblage of the two dimensional edge cracked elements; the middle surface of the plate on one side of the line spring is free to displace and rotate relative to the middle surface on the other side, as shown in Fig. 3.6. The magnitudes of separation due to the cracked region, along the middle surface of the plate is expressed in terms of a displacement δ, and a rotation θ, at any point along the crack line and are functions of the tension N and the bending moment M per unit length,

transmitted at that point. This force N and the bending moment M are related to the displacement δ and rotation θ by linear spring coefficients (compliances) called line springs. The cracking that follows the application of this tensile force and moment is called mode I cracking. The aim of the line spring model is to avoid a complete three dimensional analysis of a surface cracked component which would, if it were not cracked, be considered as a shell structure. The first step is to take into account the local loss of stiffness of the shell due to the part-through crack. To evaluate the additional compliance generated by the crack, a comparison is made between a cracked and an un-cracked strip under plane strain conditions. For a given loading (N, M) and crack geometry (a, t, H), the deformation of (δ, θ) caused by the crack is defined as:

$$\delta_c = \delta - \delta_{nc} \qquad (3.12)$$

$$\theta_c = \theta - \theta_{nc}$$

where the subscripts c and nc stand for a crack and no crack situation. δ_c and θ_c refer to displacements in the crack plane, which can be expressed in terms of the end moments and forces by means of a compliance matrix **C**; **C** is a function of (a/t), and represents the influence of the crack on the local stiffness of the shell. Parameters a, t and H are the crack depth, plate thickness in the direction of the crack and the distance of the crack respectively, from the loaded end as shown in Fig. 3.6.

$$\begin{bmatrix} \delta_c \\ \theta_c \end{bmatrix} = [\![\mathbf{C}]\!] \begin{bmatrix} N \\ M \end{bmatrix} \qquad (3.13)$$

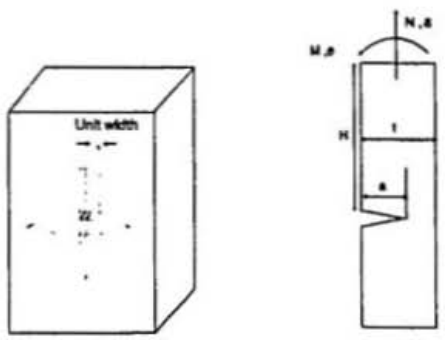

Fig. 3.6 The crack mode I for using line spring element

The first assumption in the line spring element is that the surface crack can be represented as a continuous line of springs, having bending and tension stiffnesses that depend on the local crack depth. The second assumption is that at a given cross section of the part through crack, the stress intensity factor is equal to the corresponding stress intensity factor of an edge-cracked strip under the same tension and bending forces. The relationship between (N,M) and the displacements (δ_c, θ_c) for mode I deformation is given in terms of the compliance matrix **C**:

$$\mathbf{C} = \frac{2(1-\nu^2)}{E}\begin{bmatrix} \alpha_{tt} & \frac{6}{t}\alpha_{tb} \\ \frac{6}{t}\alpha_{tb} & \frac{36}{t^2}\alpha_{bb} \end{bmatrix} \tag{3.14}$$

The coefficients α_{ij} have been derived by various authors, using the energy compliance relations, which are polynomials in $X = a/t$. The relevant equations are:

$$\frac{\partial \alpha_{ij}}{\partial a} = \pi \frac{a}{t^2} F_i F_j \tag{3.15}$$

$$\alpha_{ij}(X) = X^2 \sum_{n=0}^{n} C_{ij}^{n} X^{n} \tag{3.16}$$

$$F_i(X) = X^2 \sum_{n=0}^{n} D_i^{n} X^{n} \tag{3.17}$$

C_{ij} and D_i are coefficients of the polynomial α_i and F_{ij} respectively. Such polynomials could be derived from polynomial fits of finite element results obtained for edge cracked strips with various a/t ratios, or by using the energy compliance method, [De. Langre and Ebersolt, 1987]. While considering the surface crack as that due to the assemblage of a number of edge-cracked plane strain specimens, as shown in Fig. 3.7, it must be borne in mind that the variation of the bending stresses along a single edge-cracked strip introduces transverse shear and the variation of the bending moments and axial forces between the various edge-cracked specimens introduces shear across the specimens. This will cause two additional modes of cracking known as mode II (shear) and mode III (torsion) cracking as shown in Figs. 3.8 and 3.9. Hence a proper analysis must consider all three modes of cracking. The stress intensity factors, which result from tension, shear and twisting are represented by K_I, K_{II}, and K_{III} respectively; these have been obtained by Tada (1973) and Desvaux (1985), as follows:

$$K_I = \sqrt{\pi a} \left[F_t \left(\frac{a}{t} \right) \sigma_t + F_b \left(\frac{a}{t} \right) \sigma_b \right] \tag{3.18}$$

$$K_{II} = \tau \sqrt{\pi a}\, F_{II} \left(\frac{a}{t} \right) \tag{3.19}$$

$$K_{III,Q} = 2Q\sqrt{\frac{\tan\left(\frac{\pi a}{2t}\right)}{2t}} \tag{3.21}$$

$$K_{III,T} = -24\frac{T}{t}\sqrt{\frac{\tan\psi}{2t}}\left[2\frac{\psi}{\pi} - \left[\frac{2}{\pi}\right]^2 G(\psi) - \frac{1}{2}\right]$$
$$\psi = \frac{\pi a}{2b}; \qquad G(\psi) = \int_0^{\psi} \arcsin\left[\frac{\sin\varphi}{\sin\psi}\right] d\varphi \tag{3.22}$$

where $\sigma_t = N/t$, $\sigma_b = 6M/t^2$, and $F_t(a/t)$, $F_b(a/t)$ are the tension and bending shape functions. τ is the shear stress, which could be approximated to V/t, where V is the shear force. The stress intensity factor for mode III is made up of a shear component and a twisting component whose contributions are denoted by $K_{III,Q}$, and $K_{III,T}$, where F_{II} is shape function for mode II deformation, Q and T are the shear force and twisting moments, respectively [Desvaux, 1985].

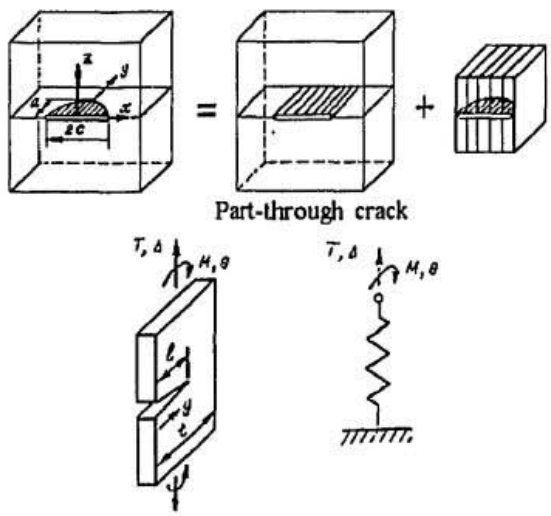

Fig. 3.7 The basic idea of the line spring model [Akimin and Nikishkov 1989]

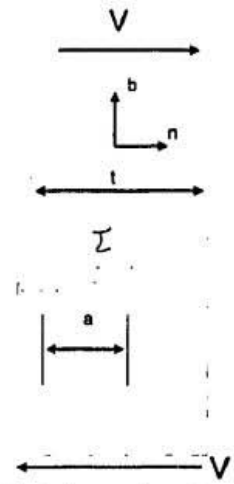

Fig. 3.8 Mode II deformation due to shear

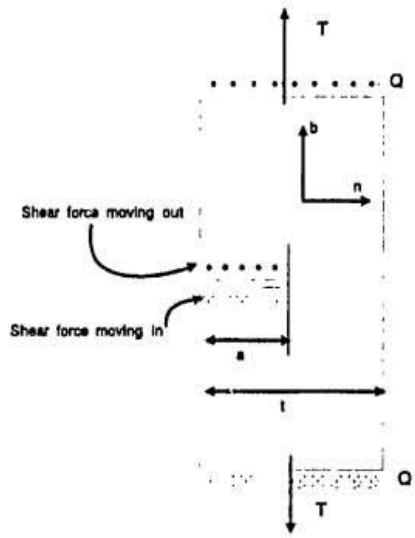

Fig. 3.9 Mode III deformation due to shear and a twisting moment

3.3.3 Implementation of the Line Spring

It has been observed that in a tubular T joint subjected to an axial tensile force, stress concentration is greatest at the saddle of the weld toe. The saddle region, being the critical one, would be the most likely location for crack initiation. Therefore, in

determining the stress intensity factors with a view to determining the fatigue life of the crack, it is important that the crack be located where the stress concentration is greatest. The line spring is used along the through-crack line between two rows of elements and represent the stiffness of a crack at that point; the line spring element will have the same nodes on either side of the through-crack line. Fig. 3.10 illustrates such a layout.

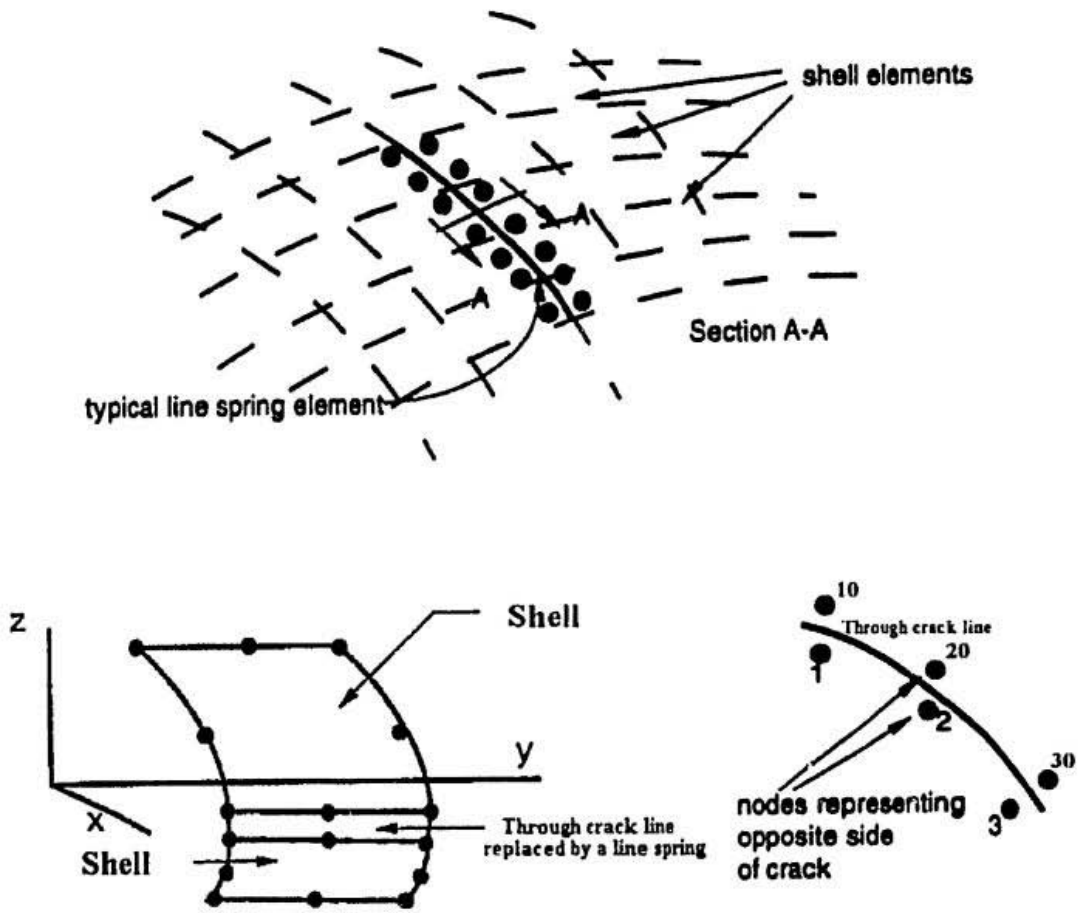

Fig. 3.10 The layout of the line spring element [Hibbitt et. al. 1989]

3.4 Fatigue Crack Growth Model

The stress intensity factors used to compute the fatigue life are those evaluated at the deepest point, which in the model occurs at the saddle. The line spring model has been shown to give excellent results for flaws which aren't too deep nor too shallow [Hibbitt et.al. 1991]. The fatigue crack growth by crack depth a and the load cycle N could be related to the stress intensity factor range ΔK by Paris' equation:

$$\frac{da}{dN} = C(\Delta K)^m \tag{3.23}$$

where C, m are crack growth constants. A typical schematic plot of da/dN vs ΔK is given in Fig 3.11. Growth law corresponding to region II would be used to evaluate propagation life of the joint. $\frac{da}{dN}$ is the change in crack depth per cycle N. The fatigue life is given by:

$$N = \int_{a_i}^{a_f} \frac{da}{C(\Delta K)^m} \tag{3.24}$$

where a_i and a_f are the initial and final crack depths, respectively.

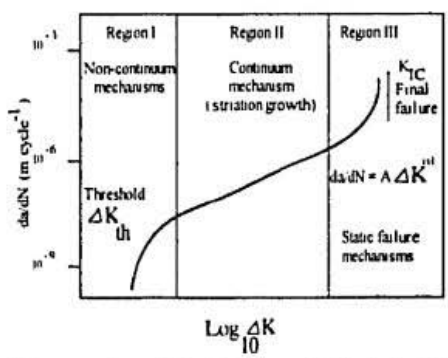

Fig 3.11 Schematic of da/dN vs ΔK plot [UEG 1985]

Chapter 4

Stress Analysis of Tubular T-Joints

4 General

The analysis of the stress and strain distributions of any structural component would help in highlighting to the designer critical design locations; in the case of a tubular T-joint subjected to axial tension, it has been shown that the weld toe region present in the T-joint intersection is the critical region and that the saddle point of the weld toe has the largest stress. Such maximum stress values have been defined in terms of parametric design equations, which have to be determined experimentally for the configuration that is of interest; such a procedure could prove to be an expensive one. A viable alternative to such a method would be to model the configuration and analyze it numerically, which is purpose of this study. Fig. 4.1 gives the configuration and the table below gives the joint parameters, of the T-joint used in this study.

Joint Parameters

Type of joint	D mm	T mm	$\beta = \frac{d}{D}$	$\tau = \frac{t}{T}$	$\gamma = \frac{D}{2T}$	$\alpha = \frac{2L}{D}$
Tee	508	6.35	0.5	1	40	7.2

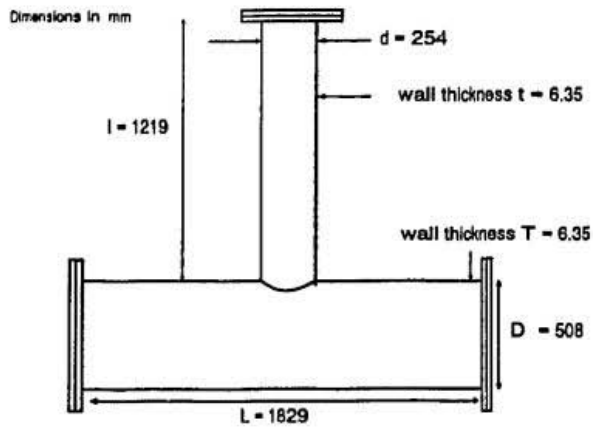

Fig. 4.1 The geometry of the T-joint

4.1 Mesh Generation

The mesh for the tubular joint was generated using the features made available in the "ABAQUS" finite element program. The joint itself consists of three components, namely, the plug, chord, and brace. Fig. 4.2 shows the model components of a tubular T-joint.

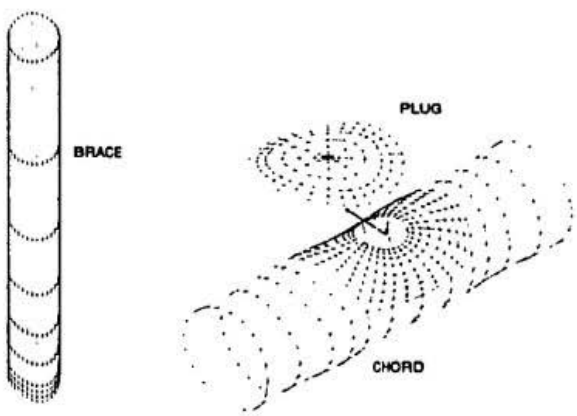

Fig. 4.2 Model components of the T-joint

It is somewhat obvious that while a fine and uniform discretization would yield good results, the problem itself would become computationally inefficient and unwieldy. Such considerations would lead to suggest that a discretization in which a fine mesh is obtained in an area of interest and a coarse one elsewhere, would be optimal; hence a fine mesh was used in the weld toe area. The aspect ratio of these elements around the weld toe, was maintained at near unity. The aspect ratio is the ratio of an element's height to its length. Care was also taken to avoid excessive distortions of the elements away from critical areas, which would lead to erroneous results. The transition from a fine mesh to a course one, was made to be gradual. The curved surface of the chord was developed in a local coordinate system as a rectangular planar surface and then mapped as a cylindrical surface to the global coordinate system. The chord and plug were discretized to having a fine mesh near the weld toe with the degree of fineness diminishing from it gradually, as one moved away from the weld toe. The plug and chord consisted of two regions of mesh. The first region "A" consisted of the mesh between the plug and an almost square region with circular arcs for its sides. The second region "B" was the mesh between such a square and the edges of the rectangle. Fig. 4.3 shows such a layout.

The brace was generated as a cylindrical surface in the global coordinate system with similar modelling considerations in mind. The half model was developed first, from which the full model was derived using the features for copying nodes and elements. The half model was used to analyze symmetric behaviour and the full model

was used to study asymmetric behaviour. Three types of elements were used to model the joint; the eight noded isoparametric element with five degrees of freedom per node, and the six noded shell triangular element with five degrees of freedom per node. The six noded line spring element was used to model the crack.

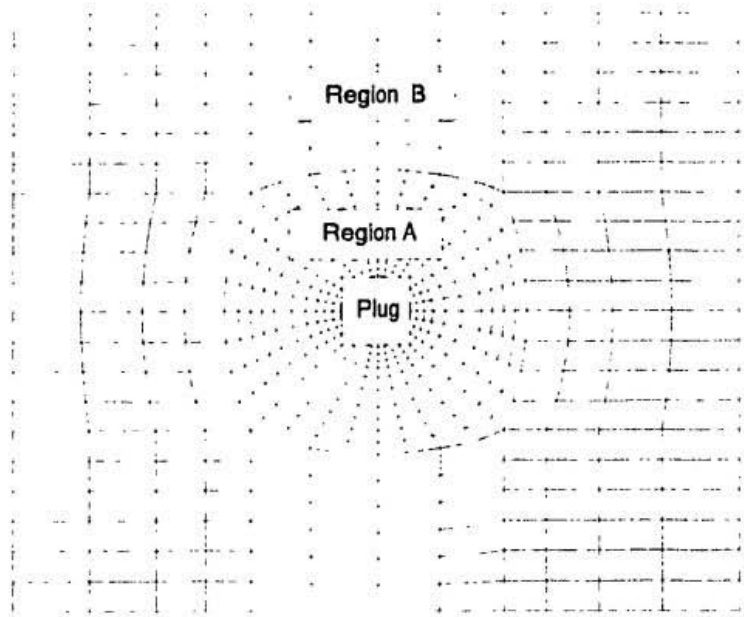

Fig. 4.3 The finite element discretization of the chord

4.1.1 Boundary Conditions

For the half model, all nodes at the end of the chord were constrained i.e., all the degrees of freedom for such nodes were made to equal zero. The nodes on either side of the brace and top and bottom-most generators of the chord were constrained to possess symmetry about a plane perpendicular to the Y axis, which in terms of the degrees of freedom are; $u_x = u_y = u_z = \phi_y = \phi_x = \phi_z = 0$ and $u_y = \phi_x = \phi_z = 0$,

respectively. The nodes at the top end of the brace, upon which the axial load bears, were constrained for rotational degrees of freedom. The full model of the tubular joint was also constrained similarly, except that the side nodes of the brace did not warrant any boundary conditions.

4.1.2 Loading

The axial load was applied as a tensile and concentrated load at each node to the top most nodes of the brace, according to the following equation:

$$F \int N_i \, dx = \frac{F l}{6} \begin{Bmatrix} 1 \\ 4 \\ 1 \end{Bmatrix}$$; where $F = \sigma_0 t$ is the force acting on an unit element, N_i is the shape function for a quadratic element and l is the length of an element, along which the load acts. σ_0 is the applied stress in the top of brace.

4.1.3 Convergence

Convergence tests were carried out to determine an optimum number of divisions at the intersection. It was found that stress concentration factors obtained for sixteen divisions at the intersection - for the quarter model, compared favourably with the results obtained using twenty four, thirty two and forty divisions. The results are given in Fig. 4.4. These results were also generated for the tubular T-joint used in an earlier experimental program [Munaswamy et. al. 1987] and the experimental values compared with the values obtained. Fig. 4.5 shows the computed and experimental values.

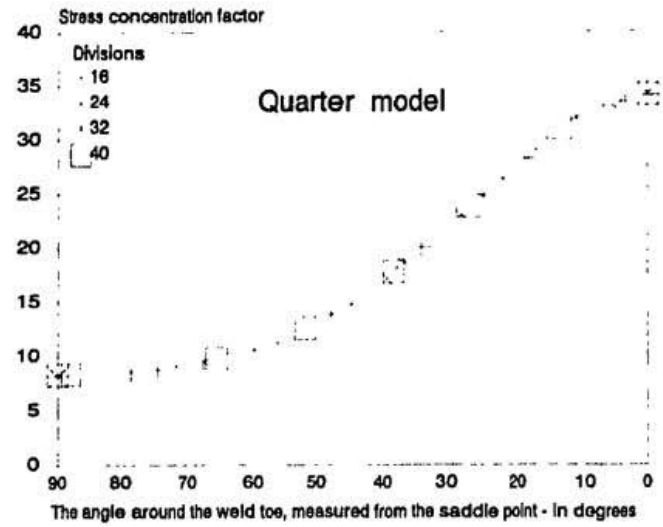

Fig. 4.4 The stress concentration factors obtained for various divisions around the weld toe

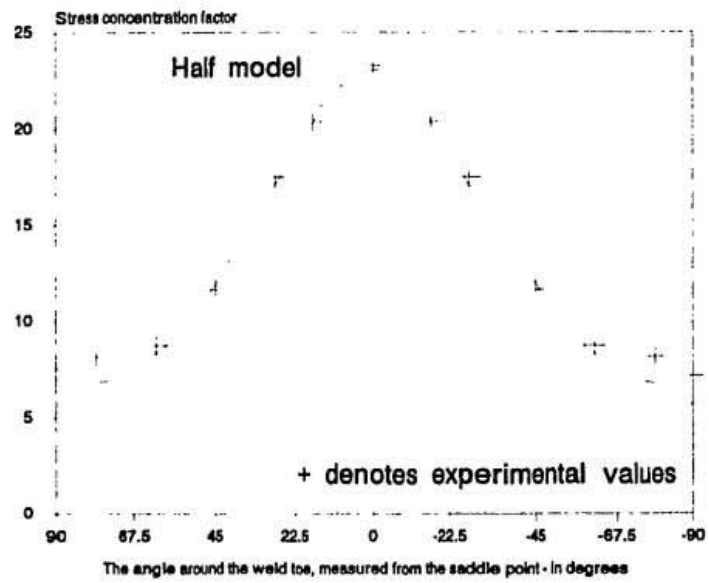

Fig. 4.5 The computed stress concentration factors for an earlier test model Munaswamy et.al. [1987]

4.2 Stress Analysis of a Tubular Joint

The stresses around the joint are analyzed to determine the regions of high

stresses where a crack would most likely grow although the presence of a crack would depend on a number of other factors. Stresses arise from three main causes:

1) The nominal stress; this is the response of the joint to the applied load.

2) Deformation stresses; these stresses arise to maintain continuity at the intersection as the tubular walls deform.

3) Notch stresses; these stresses are introduced at a geometrical discontinuity, such as that found in the welded and cracked regions.

Nominal Stresses

Nominal stresses are the stresses applied to the member (in this case, the brace) due to the externally acting loads. Depending on whether the applied load is an axial or bending load, the magnitude of the nominal stress is computed by dividing the applied load or moment, by area or sectional modulus, as the case may be.

Deformation Stresses

In a tubular joint subjected to an axial load, the tendency to deform is more at the saddle than at the crown for a given axial load. This allows a greater portion of load to be distributed to the saddle region, which is necessary to maintain structural continuity. Thus, the stiffness varies from crown to saddle, which gives rise to a maldistribution of stresses around the weld toe region as shown in Fig. 4.6.

Notch Stresses

Notch Stresses are the result of a geometric discontinuity in a tubular T joint. The section changes abruptly at the weld toe, which gives rise to notch stresses (UEG 1985). Fig. 4.6 shows the maldistribution of stresses in a typical T-joint under an axial tensile load.

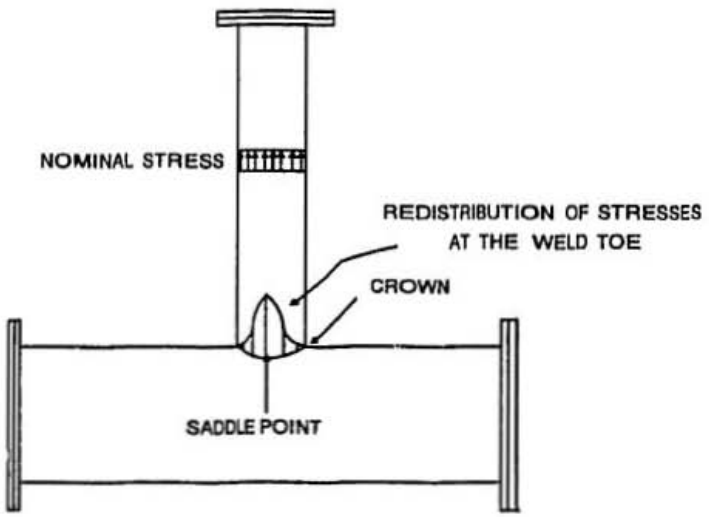

Fig. 4.6 Maldistribution of stresses at the weld toe

In analyzing the stresses around the weld toe, three situations have been considered:

1) The stress distribution in the absence of a crack

2) The stress distribution in the presence of a symmetric crack

3) The stress distribution in the presence of an asymmetric crack

4.2.1 Stress intensity factor evaluation

It would seem reasonable to model the line-spring where the stress concentration factors derived from the finite element computation compare closely with those obtained

from parametric formulae. The parametric stress concentration factors could not be determined for the joint since the parameter γ did not fall within the prescribed limits for which the most of the available formula held good; hence a comparison was not available for the SCF computed for the joint. Thus, the line-spring elements were modelled at the intersection, where the stress concentration factor was greatest, as shown in Fig. 4.7.

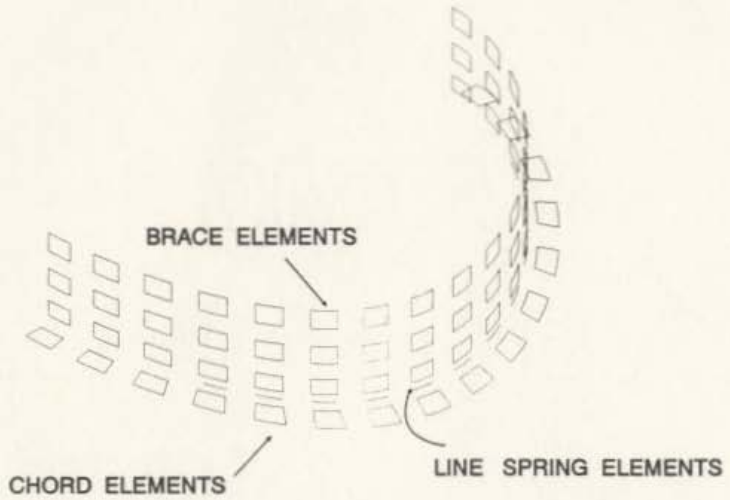

Fig. 4.7 Line-spring elements at the intersection

The line spring element was used in this study as the finite element idealisation for modelling a semi-elliptical crack. Twelve elements were placed symmetrically about the saddle point at the intersection to represent the crack. The crack was modelled on the shell surface with the depth of the crack perpendicular to the surface. The crack was defined as being positive or negative according to the convention shown in Fig. 4.8.

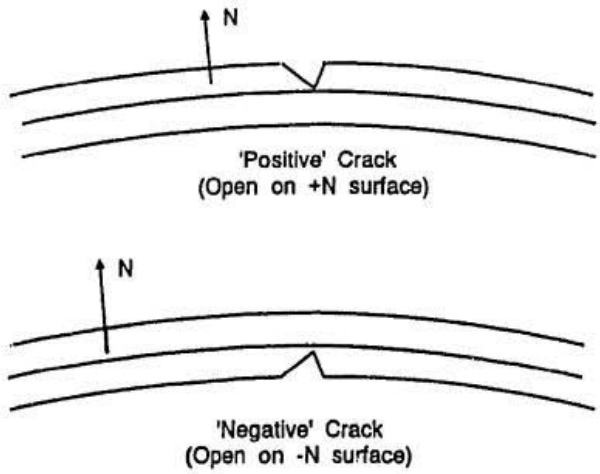

Fig. 4.8 Sign convention for crack orientation

The method by which the line spring is made to be an integral part of the model is shown in Fig. 3.7. The crack was modelled as a semi-elliptical crack whose major axis equalled the length of the chord joining the two extremities of the crack. The projection of the length between nodes at the intersection on the major axis was taken to be the position along the axis, for which the depth was calculated.

The stresses obtained were given in a local coordinate system, whose local axis S_{11} at a given point is defined as the projection of the global x axis onto the shell surface. S_{22} is derived in such a manner that the normal to the surface and S_{11}, i.e., the projection of the global x axis onto the surface form a right handed orthogonal coordinate system. Should the global axis be normal to the shell surface, the local 1 - direction is taken to be the projection of the global z axis onto the shell surface. Fig. 4.9 shows such an arrangement.

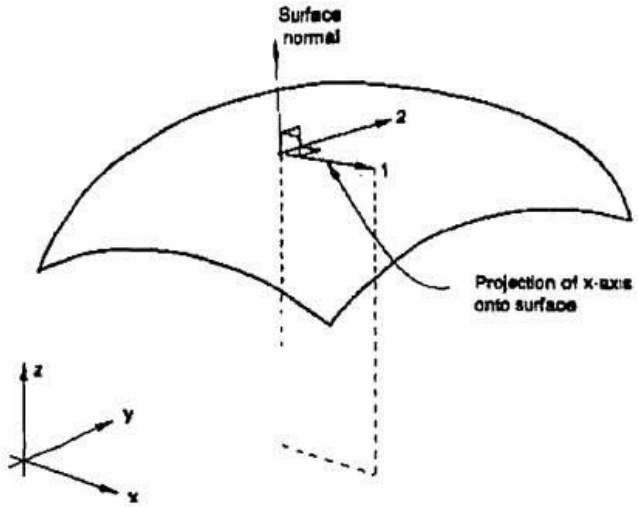

Fig. 4.9 The orientation of the local 1-2-3 axes

To compute the radial and tangential stresses, an expression was derived for the angle β between a radial line emanating from the plug and the generator of the chord given by:

$$\arccos\left[\frac{\lambda\sin\theta\cos\phi}{\sqrt{R^2+\lambda^2\sin^2\theta\cos^2\phi}}\right]$$; where R, r, θ, and ϕ, are as shown in Fig. 4.10, and $\frac{R}{\cos\theta} = \frac{r}{\sin\phi} = \lambda$

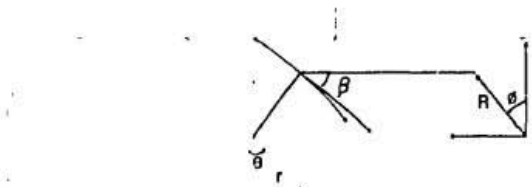

Fig. 4.10 The definition of the angle β

4.3 Results and Discussion

The stress concentration factors for the T-joint were computed for the brace and chord respectively. It was clear that the chord had the larger stress concentration factors than the brace, which meant that the crack would initiate at the chord weld toe region of the intersection, Fig. 4.11. Hence, only the stresses at the chord end of the intersection would be of interest.

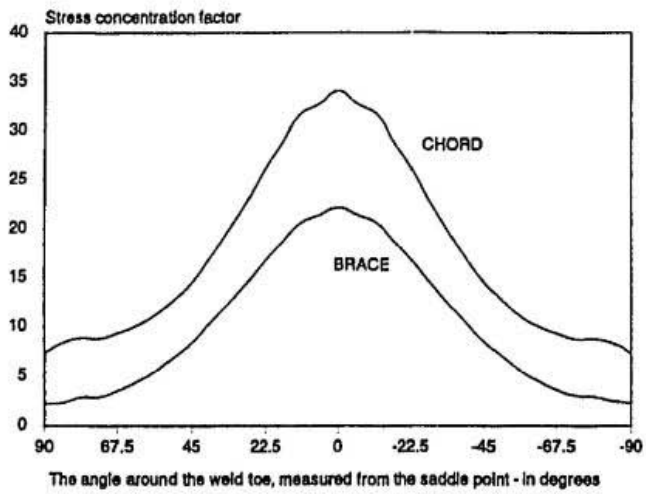

Fig. 4.11 Stress concentration factors for uncracked chord and brace

The radial and tangential stresses were the preferred stresses to work with instead of the principal stresses, because it was deemed that in dealing with the principal stresses, the stress orientation would need to be known; this would leave one with less physical insight into the stress distribution than a stress system based on a curvilinear system that would take into account the geometry of the configuration. For the symmetric case the radial stresses at the intersection reduced greatly as the crack grew in depth around the weld toe region, while the tangential stresses increased with

increasing crack depth as shown in Figs. 4.12 and 4.13, respectively.

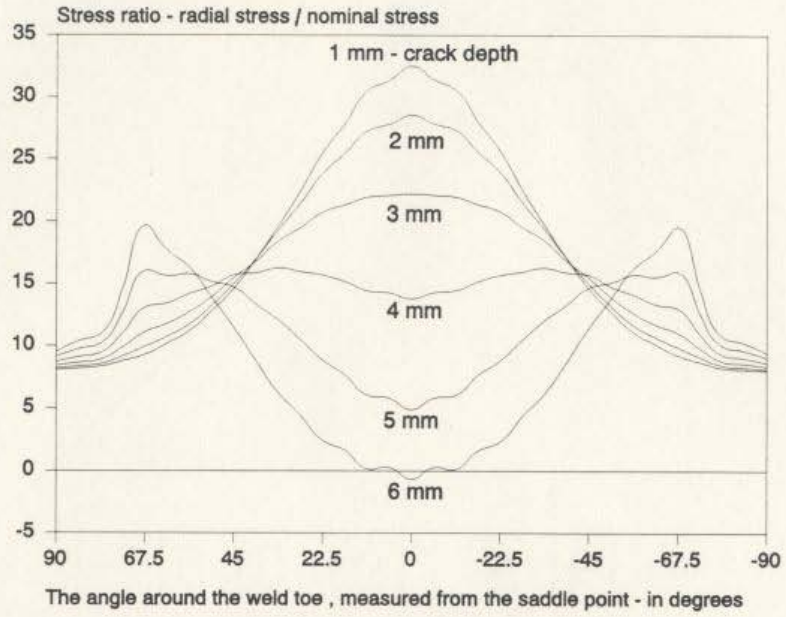

Fig. 4.12 Radial stresses at the intersection, for various crack depths

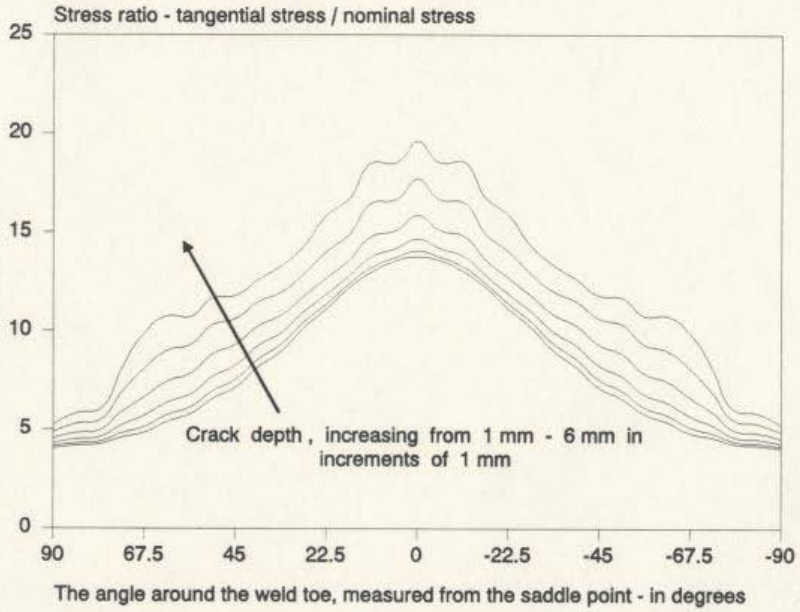

Fig. 4.13 Tangential stresses at the intersection for various crack depths

The tangential and radial stresses for the asymmetric case were observed to be similar

to the symmetric situation for the cracked side, whilst the radial and tangential stresses on the uncracked side decreased with increasing crack depth as shown in Figs. 4.14 and 4.15.

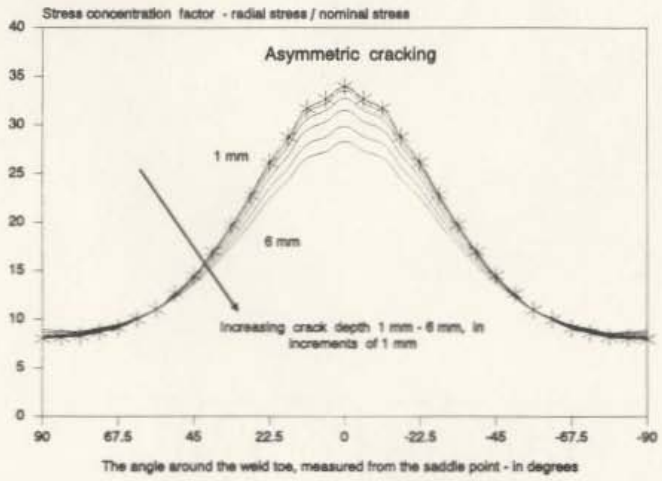

Fig. 4.14 Radial stresses around the weld toe on the uncracked side

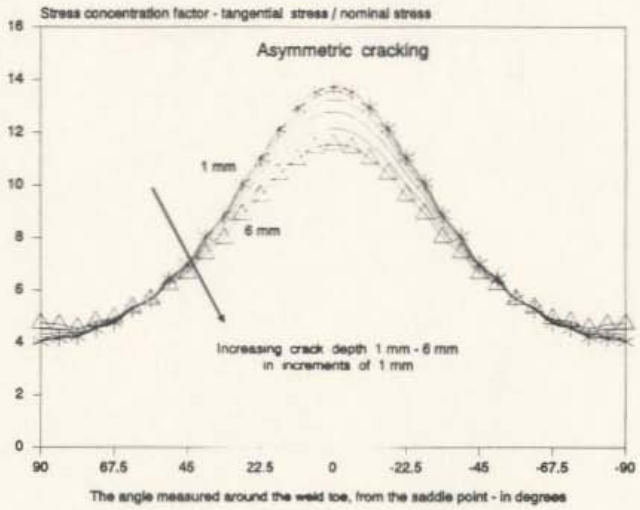

Fig. 4.15 Tangential stresses around the weld toe on the uncracked side

2The Mises equivalent stress, which gives an indication of the tendency to crack increased progressively at distances away from the saddle point (along the greater circle) as shown in Figs. 4.16 and 4.17 respectively, for the symmetric and asymmetric cases. For the symmetric case, near the crack site the Mises equivalent stress along the weld toe reduced gradually till a certain crack depth (between 4-5 mm) and thereafter increased, as seen in Fig. 4.18; this is due to the decrease of the radial stress and the corresponding increase of the tangential stress at the saddle region, as shown in Figs. 4.12 and 4.13. Additionally, this increase towards the later stages of crack growth also indicates the increased influence of shear stresses at the crack region, leading to dominance of K_{II} and K_{III} values, as shown in Fig. 4.19 and 4.20.

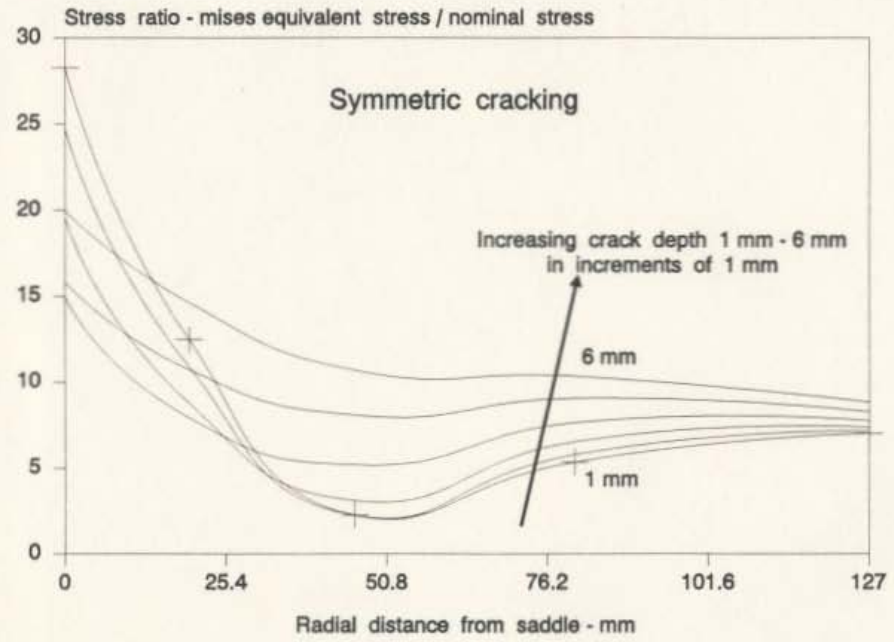

Fig. 4.16 The variation of the Mises equivalent stress ratio away from the saddle point, along the chord

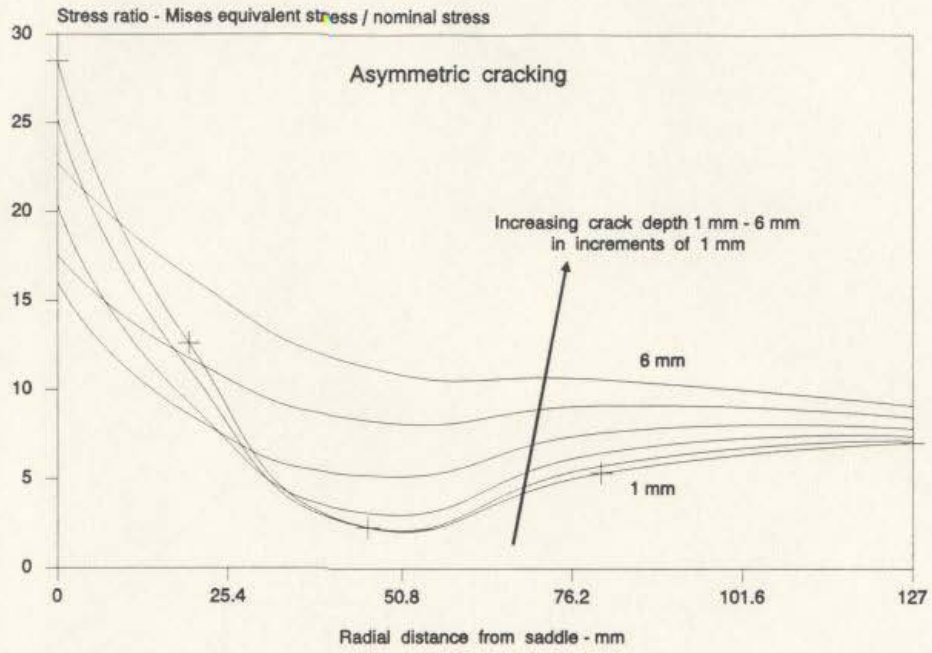

Fig. 4.17 The variation of the Mises stress ratio away from the saddle point along the chord.

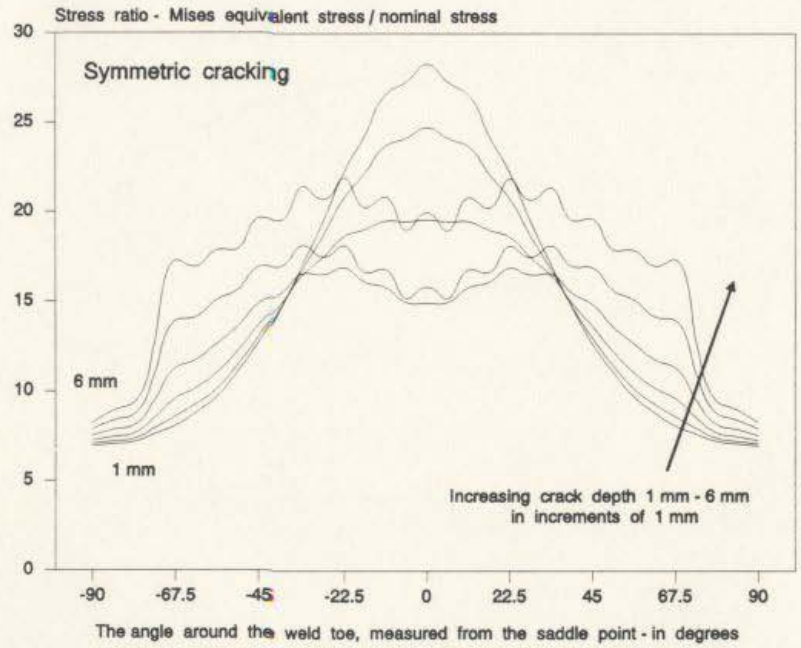

Fig. 4.18 The variation of the Mises equivalent stress along the intersection

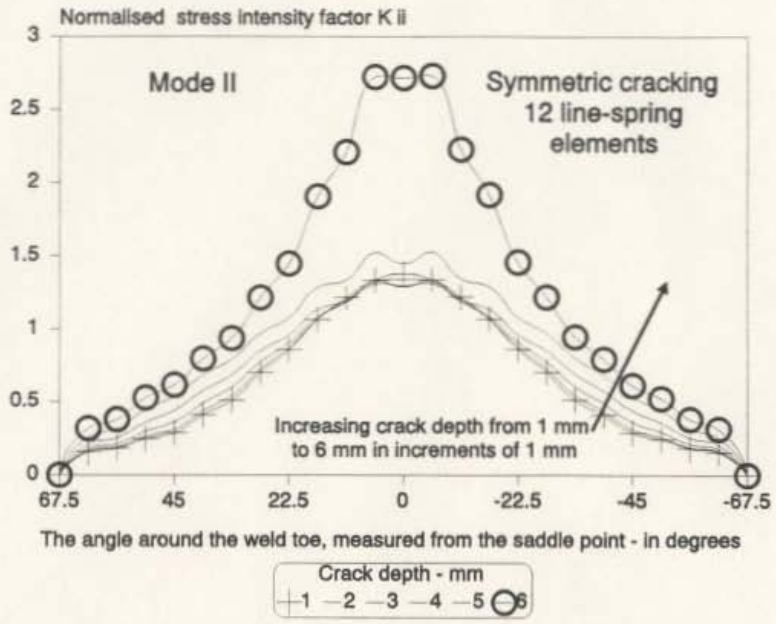

Fig. 4.19 SIF mode II variation along the crack front (Normalized SIF $K_{II}=K_{II}/\gamma_{nom}(\pi a_0)^{1/2}$)

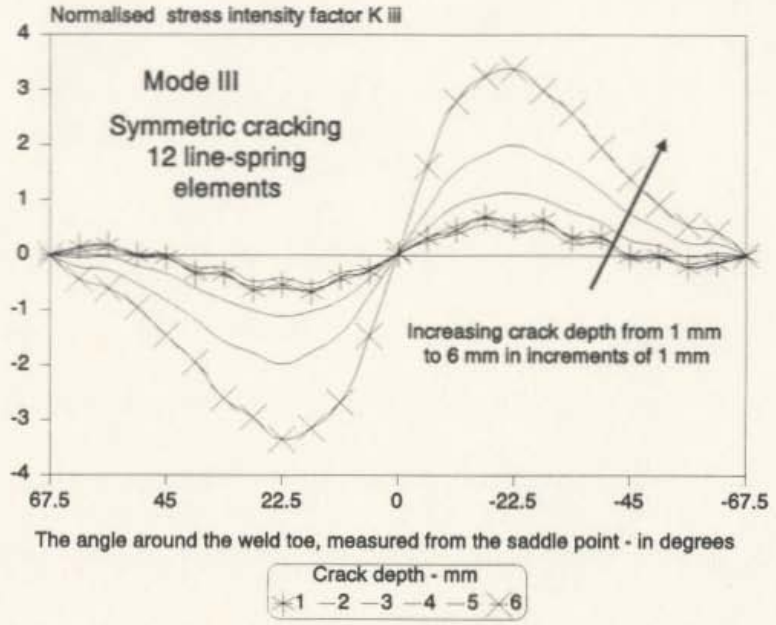

Fig. 4.20 SIF mode III variation along the crack front (Normalized SIF $K_{III}=K_{III}/\gamma_{nom}(\pi a_0)^{1/2}$)

The variation of the Mises equivalent stress for the un-cracked side, for the asymmetric cracking situation is given in Fig. 4.21. As the crack depth increases on the opposite side, the Mises stress decreases uniformly on the un-cracked side, decreasing its tendency to crack.

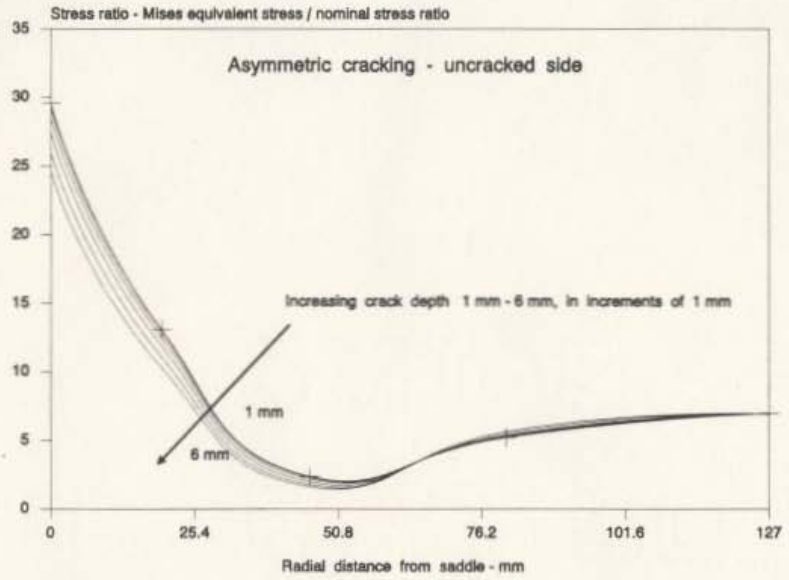

Fig. 4.21 The variation of the Mises equivalent stress ratio away from the saddle point on the un-cracked side

The predominant mode of crack advance was observed to be the K_I for the symmetric and asymmetric cases; hence only K_I was considered in calculating the propagation life of the joint. It was observed that K_I was greatest at the saddle point, until the crack reached a particular depth, after which the K_I value for the saddle point decreased as the crack advanced. This pattern was observed for both the symmetric and asymmetric cases. The variation of K_I for symmetric cracking at the weld toe is shown in Figs. 4.22 and 4.23. This observation was taken to mean that the energy available for fracture or crack growth through the thickness decreased at the saddle region, while the energy

available for crack growth along the weld toe increased; nevertheless the stress intensity factors at the extremities of the crack were observed to be always lower than those obtained for intermediate points, which suggests that the dominant SIF region could probably be along some other direction going into the chord than along the weld toe. Similar observations could be made for stress intensity factors obtained for asymmetric cracking.

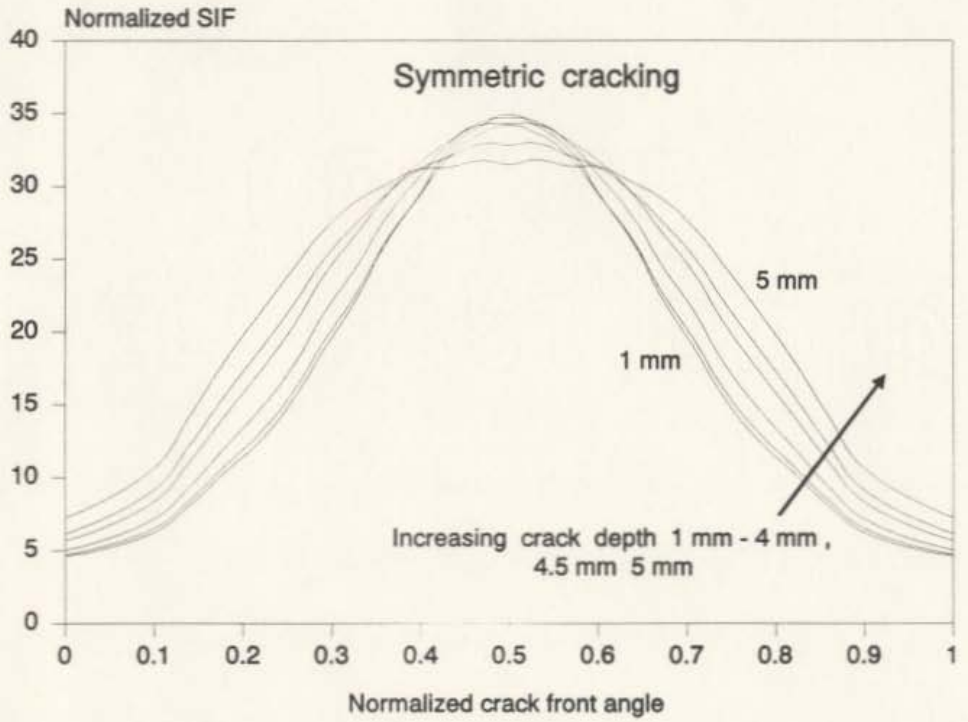

Fig. 4.22 SIF Mode I variation along the crack front (Normalized SIF = K_I / σ_{nom} $(\pi a_0)^{1/2}$).

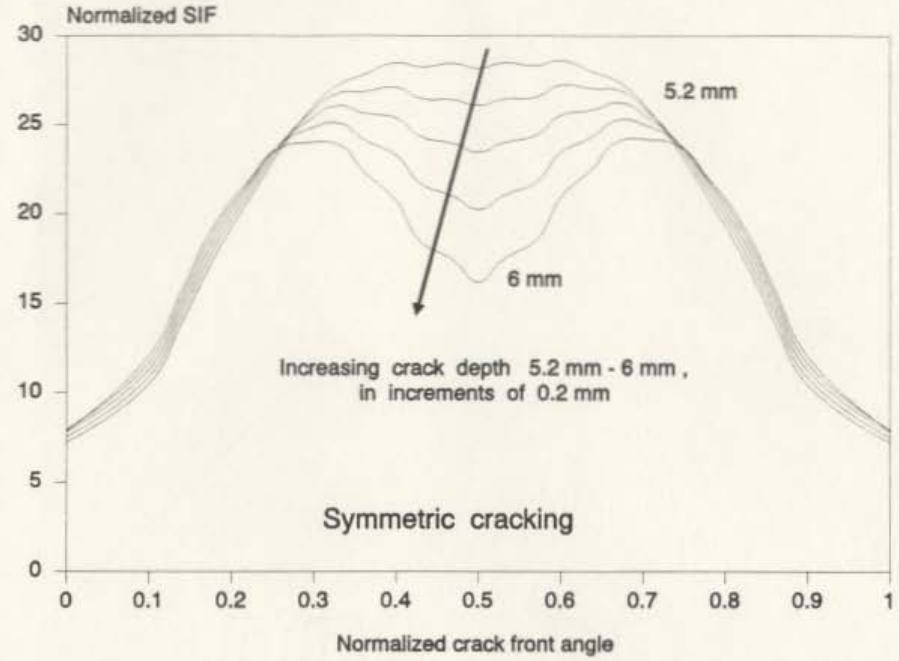

Fig. 4.23 SIF Mode I variation along the crack front (Normalized SIF = K_I / σ_{nom} $(\pi a_0)^{1/2}$).

The SCF on the un-cracked side decreased very gradually for the asymmetric crack as shown in Fig. 4.24. SIF's obtained for asymmetric cracking were equal to those obtained for symmetric cracking. For relatively smaller crack depths, the SIF's for the asymmetric situation increased with increasing crack depth, as shown in Fig. 4.25. It is clear from Fig. 4.25 that the difference in the SIF's for the two cases increases as the crack depth increases with the asymmetric crack front having the higher SIF values, which accounts for a shorter propagation life for an asymmetric crack. The crack growth behaviour, or the manner in which the SIF's vary for the two cracking situations is similar. The slight drop in the SCF values (Fig. 4.24) for the asymmetric situation could be consequential to the redistribution of stresses around the weld toe, due to the stress relieving that takes on the crack side, as the crack advances.

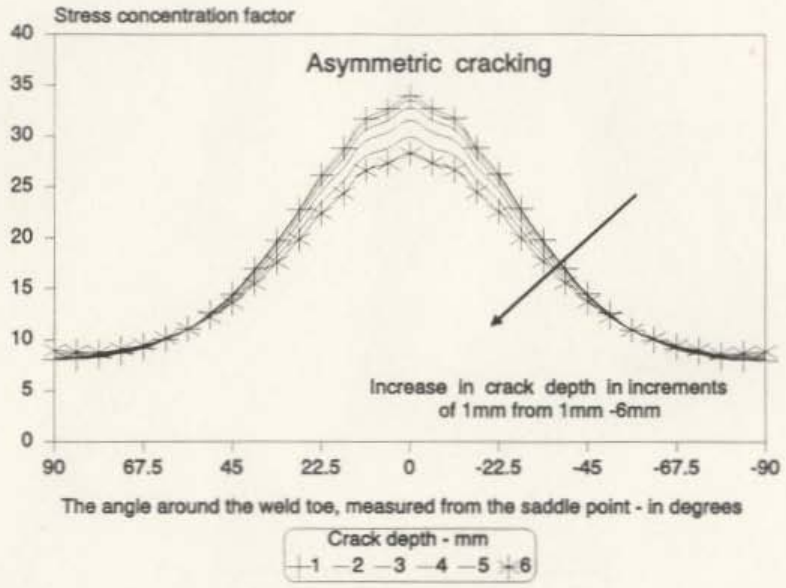

Fig. 4.24 The variation in the SCF's on the un-cracked side - asymmetric cracking

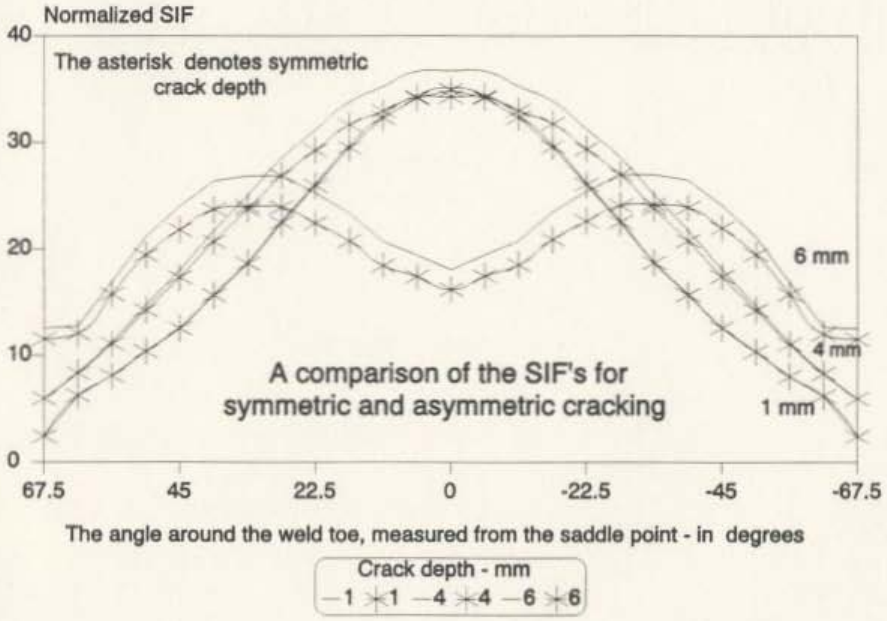

Fig. 4.25 A comparison of the SIF's for symmetric and asymmetric cracking

The deformation of the brace and the chord for symmetric and asymmetric cracking are shown in Figs. 4.26 to 4.28. It is seen that the brace remains straight for symmetric cracking, while it inclines towards the uncracked side for asymmetric cracking.

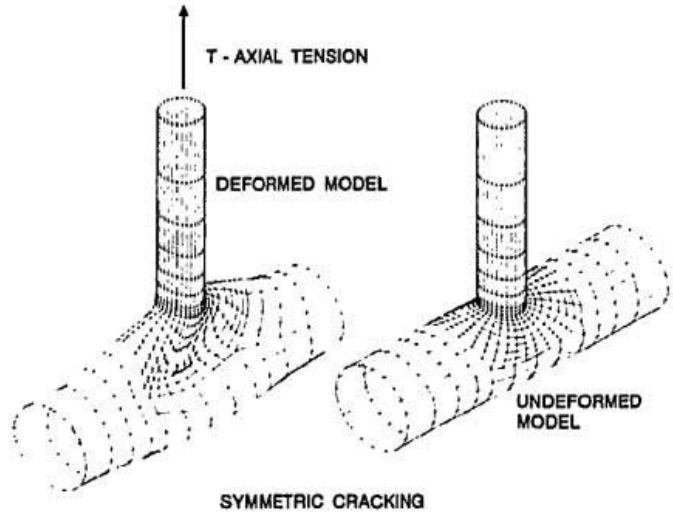

Fig. 4.26 Deformation of model - symmetric cracking

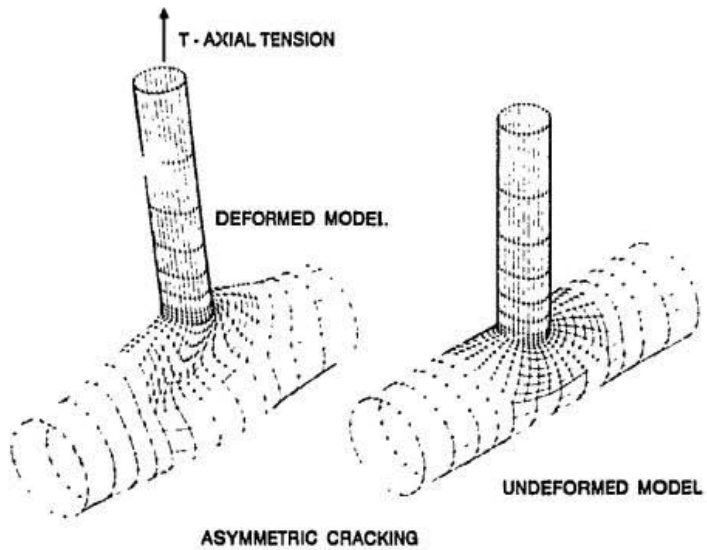

Fig. 4.27 Deformation of model - Asymmetric cracking

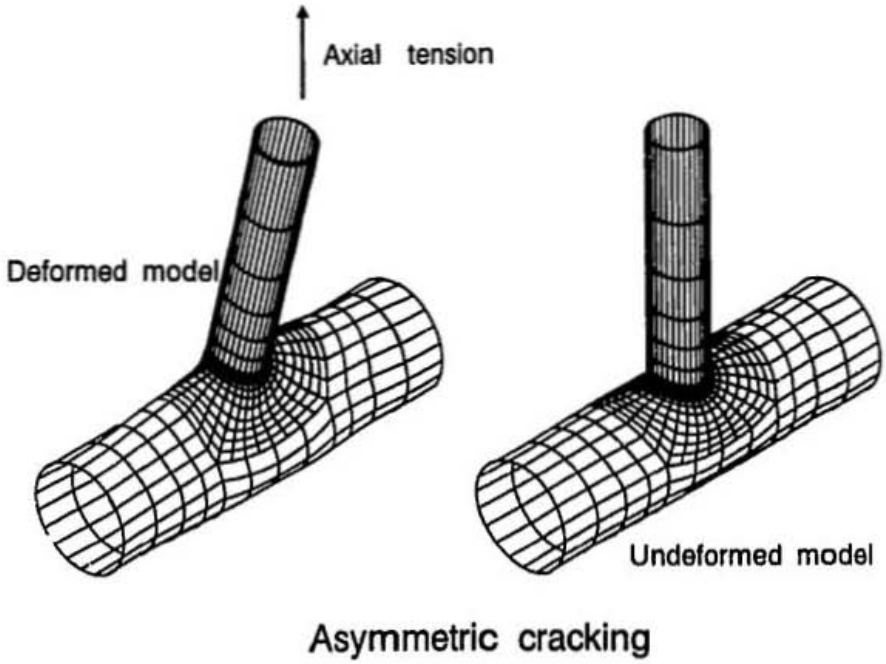

Fig. 4.28 View from the uncracked side of joint, for the case of asymmetric cracking

Chapter 5

Fatigue Life Prediction

5.1 Crack Initiation and Propagation Lives

In the traditional fracture mechanics approach to fatigue crack growth, it is assumed that an initial defect already exists and that fatigue life is made up of the propagation alone. A clearer understanding of fatigue could be had, if the fatigue life is resolved into three characteristic stages of initiation, propagation, and fracture. Initiation is analyzed at the microscopic level while propagation is analyzed at the continuum level. The total fatigue life N_T is given by:

$$N_T = N_i + N_p \tag{5.1}$$

where N_i = Number of fatigue load cycles for crack initiation, and N_p = Number of fatigue load cycles for crack propagation. Crack initiation cannot be defined precisely. For discontinuously jointed components like welded joints, it is usually assumed that N_i is the number of cycles within which a crack of an initial size - usually of the order of tenths of a mm - grows. It has been observed that the crack initiation life becomes significant in the total life of the joint only in the event of small wall thickness, low fatigue stress range, post weld improvements etc. The Manson Coffin's equation (5.2) will be used to determine the initiation life. The four coefficients required for this analysis viz., σ'_f , ϵ'_f, b, and c are coefficients whose values were determined using the

plot shown in Fig. 5.1 for crack initiation life obtained by (Iida 1987) for several T-joint configurations. σ'_f is the fatigue strength coefficient, b is the fatigue strength exponent, c is the fatigue ductility exponent, ϵ'_f is the fatigue ductility coefficient, $2N_f$ is the reversals to failure or the initiation life, $\Delta\epsilon$ is the total strain amplitude, and E is the modulus of elasticity. Manson Coffin's equation is given by:

$$\frac{\Delta\epsilon}{2} = \frac{\sigma'_f}{E}(2N_f)^b + \epsilon'_f(2N_f)^c \tag{5.2}$$

This equation is solved by a combination of the results from finite element analysis, which gives the strain at the critical hot-spot region, and the use of existing data for crack initiation in thin walled tubular joints. It is assumed that the strain component obtained from the elastic numerical analysis is almost the same as the total strain used in Eqn. (5.2).

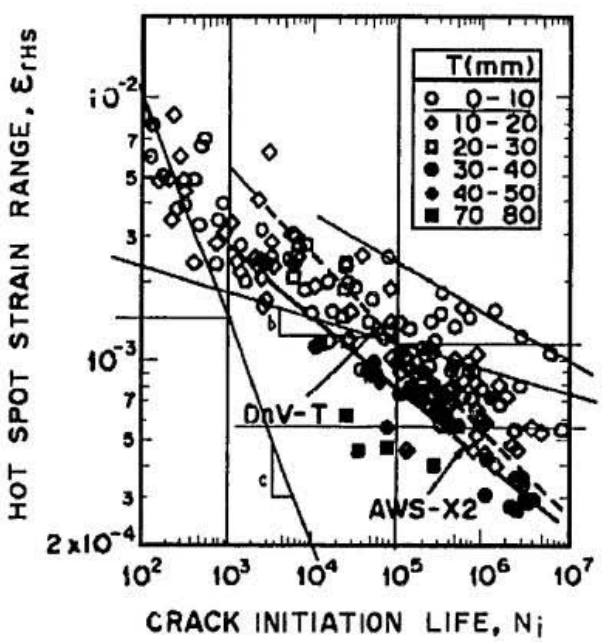

Fig. 5.1 Crack initiation life

The coefficients required to compute the initiation life were determined using the results given in Fig. 5.1. In the high reversals to failure range, i.e., 10^5 - 10^7, a mid-range line (for thicknesses ranging from 0 - 10 mm) was determined from the upper and lower bound lines. This line was taken to represent the elastic strain of a T-joint having a chord thickness between 0 - 10 mm. The gradient of the elastic line and the intercept would give the two coefficients b and σ'_f, respectively. In the lower reversals to failure range, i.e., 10^2 - 10^3, the mid-range line was bounded by the upper and lower bound lines and was constructed to give a steep slope, as much as was possible whilst not deviating in excess of the exact mid-range line; the reason being that for most ductile steels $\epsilon'_f \approx 1$, and for strong steels $\epsilon'_f \approx 0.5$ (Bannantine et.al., 1990). However, it was observed in this situation that the best possible slope yielded a value of 0.1125 for ϵ'_f, which is a little low. The values for the coefficients σ'_f, b, and c were 396.64 MPa, -0.0985 and -0.699, respectively.

5.1.1 Propagation life

Growth rate of a fatigue crack is governed by changes in the stress intensity factor at the critical cracked region. The equation proposed by Paris and Erdogan (1963) would be used to determine the propagation life of the crack, viz.,

$$\frac{da}{dN} = C(\Delta K)^m \tag{5.3}$$

where $\Delta K = K_{max} - K_{min}$, with K_{max} and K_{min} referring to the maximum and minimum values of the stress intensity factors in the critical hot-spot region of the welded zone during the fatigue load cycle.

If da/dN versus ΔK for a crack is plotted on a logarithmic scale an approximately sigmoidal curve results, as shown in Fig. 5.2.

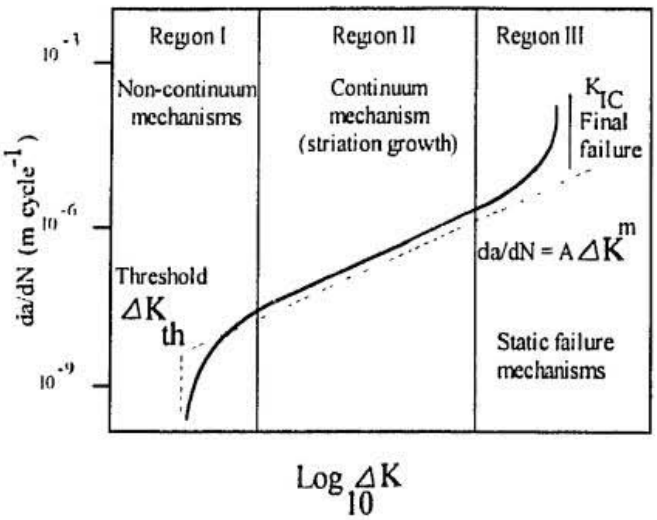

Fig 5.2 Schematic da/dN Vs ΔK plot

The constants C and m are determined empirically from a plot of $\log(\Delta K)$ vs. $\log\left[\frac{da}{dN}\right]$. The value of m is usually in the range of $2.5 \leq m \leq 4.5$ for welded steel, and is usually assumed to be equal to three, while C is a material constant. Paris' equation does not however account for the crack growth behaviour at low and high levels of ΔK. For example it is possible for a crack not to advance if the value of ΔK is less than the threshold value. If there are a high proportion of cycles near the threshold, the crack growth predictions will be conservative and an adjustment would have to be made. The Paris equation should not be used if there are a large number of cycles at high stress intensity values, e.g., $K_{max} > 0.7\ K_{IC}$.

To calculate the absolute fatigue life by fracture mechanics requires more caution [UEG 1985]. To use appropriate values for C and m, the relationship obtained by

[Gurney 1979] has been used, where C and m are related by the following equation:

$$C = \frac{1.315 \times 10^{-4}}{895.4^{m}} \tag{5.4}$$

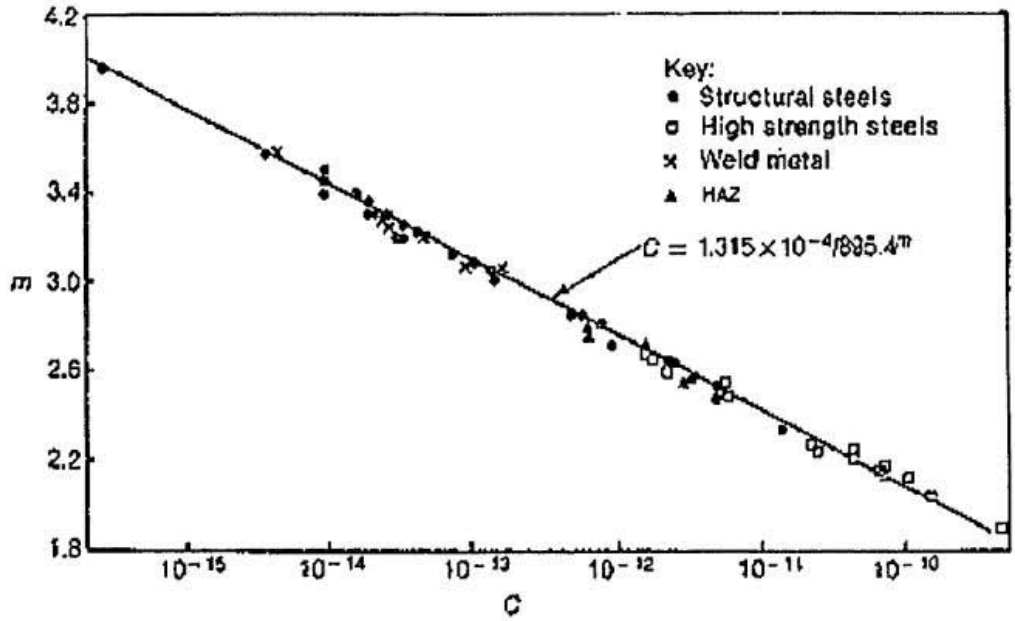

Fig. 5.3 Shows the relationship between the fatigue life coefficients C and m

Several values have been suggested for the material constants C and m, based on the various factors that would affect the material composition and stress state of the joint such as the metal microstructure, marine fouling, cathodic protection, mean stress, and fatigue thresholds [UEG 1985]. For this study, the values computed for C and m are 1.832×10^{-13} and 3.0, respectively. In computing the propagation life the maximum crack depth was incremented by 0.2 mm, starting from 0.2 mm up to 6 mm, which means that an initial defect of 0.2 mm has been assumed. The difference between the stress intensity factors was taken to be ΔK, for which the propagation life was computed. Fig. 5.4 shows the fatigue life obtained for the symmetric and asymmetric cases.

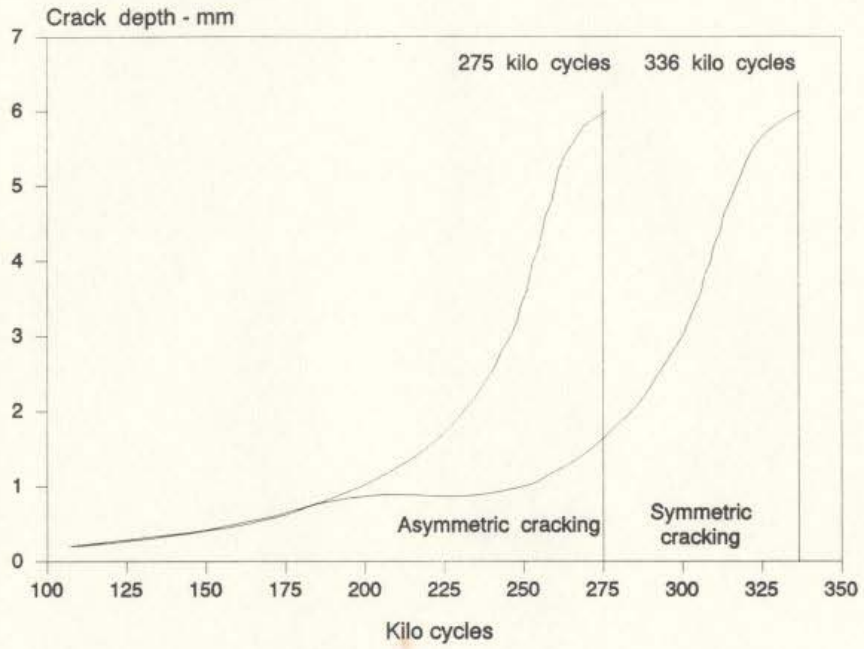

Fig. 5.4 Crack propagation life ($x10^3$ cycles)

5.2 Discussion of results

Table A gives a comparison of the computed and experimental values obtained for the initiation and propagation lives. The experiment was done towards the Ph.D. thesis work of a fellow graduate student (Ms. Cheng Shumin).

Table A

Life x 10^3	Initiation	Propagation
Experimental values	600	500
Computed values	570	275

It is evident that while the initiation lives compare favourably, the propagation lives do not. The reason for a low propagation life is the fact that computed stress intensity factors are higher than the actual values. This could be substantiated by the fact that a fractional value between 0.9 and 0.8 of the computed value would yield the observed

value, as shown in table B. If it were possible to determine the parametric stress concentration factor, the crack would have been modelled in a region with a SCF value, comparable with that obtained from the parametric equation - as outlined in the paper by [Du and Hancock 1989]. This however was not possible, as the parameter γ did not come under the prescribed limits.

Table B

The propagation life in kilo cycles, for fractions of the obtained SIF Mode I				
Fraction	1	0.9	0.8	0.7
Propagation life	275	377	537	802

Two methods could be adopted to overcome the difference:

i) Place the line spring away from the intersection, e.g. one row away from the intersection; this would yield stress intensity factors lower than those obtained at the intersection.

ii) Increase the thickness of one or two rows of the brace near the weld toe to represent the weld thickness.

Chapter 6

Conclusions and Recommendations

6.1 Conclusions

A study of the fatigue life of a tubular T-joint using the linear fracture mechanics approach is presented. Since the finite element modelling preceded the experiment that is now being carried out in the structures laboratory (for Ms. Cheng Shumin), it was not possible to use the experimental values as a "check" to model the T-joint. This model was consequently used to corroborate the results of a previous experiment done by Munuswamy et. al. (1987); the computed SCF's compared favourably with the experimental values. The crack was modelled at the intersection, which with hindsight we see that, it under-estimates the actual propagation life. The crack might have been modelled away from the intersection, if it were possible to calculate the parametric SCF, as then, the crack would have been modelled in a region having a similar SCF. In the experiment, the tubular T-joint developed an asymmetric crack, which means that the comparisons made would be in reference to such a crack analyzed, numerically.

A comparison of the computed values with the experimental shows that:

1) The SCF's at the weld toe compared well with the experimental values.

2) The computed propagation life for an asymmetric cracking, was only 55% of the

experimental crack propagation life.

3) The stress intensity factor is defined as, $K = \sigma^*\sqrt{(\pi a)}^*Y$, where K is the stress intensity factor, a is the crack depth, and Y is the magnification factor. The SIF's obtained for an asymmetric crack were greater than those obtained for a symmetric crack, for the same stress and crack depth; hence it could be concluded that for a tubular T-joint, the cracking will predominantly be in an asymmetric manner.

4) In estimating the fatigue life of a tubular T-joint, the propagation life based on asymmetric crack growth would give a lower value, unless the line-spring elements are placed at the right location.

5) The local strain approach could be used to determine the initiation life of the tubular T-joint.

6) Line-spring elements could be used to determine the stress intensity factors along the crack front in structures such as tubular T-joints.

6.2 Recommendations for future research

As a continuation to the work that has been done, the following facts come across as being worthy of further study.

i) To obtain values for the stresses and propagation life, after properly modelling the first row of the brace elements at the intersection to account for the thickness of the weldment. Also the line spring element must be placed in between the first and second row of the chord element.

ii) To investigate the stresses and propagation life for other types of joints using the principles of linear fracture mechanics.

iii) To analyze the problem taking into account the effects of plasticity

iv) To carry out compact tension specimen tests and determine the values of C and m, for the material of the tubular T-joint.

Bibliography

Ahamed, S., Irons, B. M., Zienkiewicz, O. C., 1970, *Analysis of Thick and Thin shell Structures by Curved Finite Elements.* Int. J. Num. Meth. Eng., Vol. 2, 1970, pp. 419 - 451.

Akimin, S.A., Nikishkov, G.P., 1991, *Weight Function Calculation for Surface Cracks Using the Line-spring Model.* International journal of Fracture 47. pp. 241-256.

Almar-Næss, Fatigue Handbook, 1985, Published by Tapir, Norges tekniske högskole, 7034 Trondheim-NTH, Norge.

Ando, Y. and Yagawa, D., 1977, *Recent Developments in Finite Element Method of Three-Dimensional Crack problems in Japan.* Proc. Int'l. Conference on Fracture Mechanics and Technology, Hong Kong, Sijthoff and Noordhoff Publishers, Vol.2, pp. 1513-1520.

Annual Book of ASTM Standards, 1981. Standard test method for plane-strain fracture toughness of metallic materials. Part 10, E399-81, pp. 592-621

Atluri, S.N., Nakagaki, M. Kathiresan, K., Rhee, H.C. and Chen, W.H., 1978, *Hybrid Finite Element Models for Linear and Nonlinear Fracture Mechanics.* Numerical Methods in Fracture Mechanics, Proc. of the First International Conference of Swansea International Conference, Swansea, Wales, 1978, pp 52-66.

Austen, I.M. and Walker, E. F. 1977, Research Report PT-6795-8-77-A.

Bananntine, J.A., Comer, J.J. and Handrock, J. L., 1990, Fundamentals of Metal Fatigue Analysis. Prentice Hall

Barsoum, R.S., 1976, *On The Use of Isoparametric Finite Elements in Linear Fracture Mechanics.* International Journal for Numerical Methods in Engineering, Vol. 8, No.1, pp. 25-37.

Barsoum, R.S., 1976, *A Degenerated Solid Element for Linear Fracture Analysis of Plate Bending and General Shells.* International Journal for Numerical Methods in Engineering, Vol. 10, No.1, pp. 551-564.

Barsoum, R.S., 1977, *Triangular Quarter-Point Elements as Elastic and Perfectly-Plastic Crack Tip Elements.* International Journal for Numerical methods in

Engineering, Vol.11, pp. 85-98.

Beale, A. and Toprac, A.A., 1967, *Analysis of In-Plane T, Y and K welded Tubular Connections.* Welding Research Council, Bulletin 125, October.

Bell, R. and Vosikovsky, O., 1992, *A Fatigue Life Prediction Model for Multiple Cracks in Welded Joints for Offshore Structures.* Offshore Mechanics and Arctic Engineering, Vol. III-B, Materials Engineering, ASME.

Benzley, S.E, 1974, *Representation of Singularities in the Isoparametric Finite Elements.* International Journal of Numerical Methods in Engineering, Vol.8, pp. 537-545.

Bhuyan, G.S., Swamidas, A.S.J., Vosikovsky, O., 1988, *Influence of Environmental and Mechanical Variables on Fatigue Crack Growth Rate in CSA G40.21M 350 WT Steel.* International Journal of Fatigue.

Blackburn, W.S. and Hellen, T.K., 1979, *Calculation of Stress-Intensity Factors in Three-dimensions by Finite Element Method.* International Journal of Numerical Methods in Engineering. Vol.11, pp. 211-229.

Boom, J.N. and van Fossen, D.V., 1976, *An Evaluation of The Twenty-Noded Quadratic Isoparametric Singularity Brick Elements.* International Journal of Fracture, Vol.12, pp. 161-163.

Bowness, D., and Lee, M.M.K., 1993, *Stress Fields and Stress Intensity Factors in Tubular T-Joints.* Offshore Mechanics and Arctic Engineering Vol. III-B, Materials Engineering ASME pp. 839-846.

Broek, D., 1974, Elementary Engineering Fracture Mechanics, Noordhoff, International Publications.

Bucak, O, Mang, F. and Herion, S., 1994, *Development and Propagation of Cracks in Welded Hollow Section Joints Under Uniaxial and Multi-axial Loading.* Offshore Mechanics in Arctic Engineering, Vol.3, Materials Engineering, ASME. pp. 159-166.

Burdekin, F. M., 1985, *Engineering Design Against Fracture at Stress Concentrations.* Material Science and Technology, Vol.1, pp. 487-493.

Chu, W.H., 1984, Msc. Thesis, UMIST.

de Back, J. and Vaessen, G.F.G., 1981, *Fatigue and Corrosion Fatigue Behaviour of Offshore Structures.* ESCE Convention, 7210-KB/6/602, Delft.

De. Langre, E. and Ebersolt, L., 1987, *The Use of a New Line Spring Shell Element for Elastic Surface Crack Analysis Fatigue*. Fract. Engng. Mater. Struct. Vol. 10, No. 2. pp. 153-167.

Delale, F. and Erdogan, F. 1982, *Application of Line-Spring Model to a Cylindrical Shell Containing a Circumferential or Axial Part-Through Crack*. Trans. ASME, Series E, Journal of Applied Mechanics, Vol.49, pp. 97-102.

Desveaux, G.J. 1985, *The Line-Spring Model for Surface Flaw, an Extension to Mode 2 and Mode 3*. M. Sc. Thesis, Dept. of Mech. Eng., Mass. Inst. Tech., Cambridge, Boston, U.S.A.

Dijkstra, O.D., Snijder, H.H. and van Straalen, I.J., 1989, *Fatigue Crack Growth Calculations Using Stress Intensity Factors for Weld Toe Geometries*. Offshore Mechanics and Arctic Engineering, The Hague, The Netherlands, March 19-23, pp. 137-143.

Dijkstra, O.D., van Straalen, I.J., and Noordhoek, C., 1993, *A Fracture mechanics Approach of Fatigue of Welded Joints in Offshore Structures*. Offshore Mechanics and Arctic Engineering, Vol. III-B Materials Engineering, ASME, pp. 675-680.

Dill, H.D and Saff, C.R., 1978, *Environment-Load Interaction Effects on Crack Growth*. Air force Flight Dynamics Laboratory, AFFDL-TR-78-137.

Donahue, R.J., Clark, H.M., Atanmo, P., Kumble, R., and McEvily, A.J., 1972, *Crack Opening Displacement and the Rate of Fatigue Crack Growth*. International Journal of Fracture Mechanics 8, pp. 209-219.

Dover, W.D., Kare, R.F. and Hall, M.S., 1991, *The Reliability of SCF Predictions Using Parametric Equations: a Statistical Analysis*. Proceedings of the Tenth International Conference on Offshore Mechanics and Arctic Engineering, Stavenger, Norway, pp. 453-459.

Dover, D.W. and Dharmavasan, S., 1982, *Fatigue Fracture Mechanics Analysis of T and Y Joints*. Offshore Technology Conference, Paper No.4404, Houston.

Dowling, N.E. and Begley, J. A., 1976, *Fatigue Crack Growth During Plasticity and the J Integral in Mechanics of Crack Growth*. ASTM STP 590, American Society for Testing and Materials, Philadelphia, pp. 82-103.

Dowling, N.E., 1977, *Crack Growth During low-Cycle Fatigue or Smooth Axial Specimens, in Cyclic Stress-Strains and Plastic Deformation Aspects of Fatigue Crack Growth*. ASTM STP 637, American Society for Testing and Materials, Philadelphia, pp. 97-121.

Dowling, N.E., 1979, *Fatigue at Notches and the Local Strain and Fracture Mechanics Approaches.* ASTM STP 677, pp. 247-273.

Du, Z.Z., and Hancock, J.W., 1989, *Stress Intensity Factors of Semi-Elliptical Cracks in a Tubular Welded Joint Using Line Springs and 3D Finite Elements.* Journal of Pressure Vessel Technology, Vol. III, pp. 247-251.

Efthymiou, M. and Burdekin, S., 1985, *Stress Concentrations in T/Y and Gap/Overlapped K-Joints,* Developments in Marine Technology, Vol.2, pp. 429-440.

Efthymiou, M. and Durkin, F., 1988, *Development of Stress Concentration Factor Formulae and Generalised Influence Functions for Use in Fatigue Analysis.* Offshore Tubular Joint Conference, London.

Engesvik, K.M., 1982, *Analysis of Uncertainties in Fatigue Capacity of Welded Joints.* Report Ur-82-17, Department of Marine Technology, University of Trondheim.

Erdogan, F. and Ratwani, M., 1970, *Fatigue and Fracture of Cylindrical Shells Containing a Circumferential Crack.* International Journal of Fracture Mechanics, Vol.6, pp. 379-392.

Flügge, W. 1960, Stresses in Shells Springer, Berlin 1960

Forman, R.G., Kearney, V.E. and Engle, R.N., 1967, *Numerical Analysis of Crack Propagation in Cyclic-Loaded Structures* Journal of Basic Engineering, Trans. ASME, Vol.89, pp. 459-464.

Gdoutos, E.E., 1990, Fracture Mechanics Criteria and Applications, Kluwer Academic Publishers.

German, N.D., Kumar V., and de Lorenzi, 1983, *Analysis of Surface Cracks in Plates and Shells Using the Line-Spring Model and ADINA.* Computers and Structures, Vol.17, Nos.5-6, pp 881-890.

Griffith, A.A., 1920, *The Phenomena of Rupture and Flaw in Solids.* Transactions, Royal Society of London, Ser. A. Vol. 221, p. 163.

Hall, C.A., Raymund, M. and Palusamy, S., 1979, *A Macro Element Approach to Computing Stress-Intensity Factors for Three-Dimensional Structures.* International Journal of Fracture, Vol.15, pp. 231-245.

Haswell, J. and Dover, W.D., 1991, *Stress Intensity Factor Solutions for Tubular Joints.* Offshore Mechanics and Arctic Engineering, Vol. III-B, Materials Engineering,

ASME. pp. 461-468.

Head, A.K., 1953, *The Growth of Fatigue Crack*. Philosophical Magazine, Vol.44, pp. 925-938.

Hellen, T.K., 1975, *On The Method of Virtual Crack Extensions*. International Journal of Numerical Methods in Engineering, Vol. 9, pp. 187-207.

Hellier, A.K., Connolly, M.P. and Dover, W.D., 1990a, *Stress Concentration Factors for Tubular Y and T Joints*. International Journal of Fatigue, Vol.1, pp. 13-23.

Hellier, A.K., Connolly, M.P., Dover, W.D. and Corderoy, D.J.H., 1990b, *Parametric Equations to Predict the Full Scale Stress Distribution in Tubular Welded Y-Joints*. Proc. of the First Pacific/Asia Offshore Mechanics Symposium, Seoul, Korea, pp. 281-293.

Henshell, R.D. and Shaw, K.G., 1975, *Crack Tip Elements are Unnecessary*. International Journal for Numerical Methods in Engineering, Vol. 9, 1975, pp. 495-509.

Hibbit, Karlsson & Sorensen Inc., 1994, Reference Manuals, Ver. 5.4

Hilton, P.D., 1977, *A Specialized Finite Element Approach for Three-Dimensional Crack Problems in Plates and Shells With Cracks*. Leiden, Noordhoff Int. Publishing, pp. 273-298.

Hinton, E., Owen, D. R. J., 1984, Finite Element Software for Plates and Shells, Pineridge Press, U.K.

Huang, X, Du, Z.Z. and Hancock, J.W., 1988, *A Finite Element Evaluation of the Stress Intensity Factors of Surface Cracks in a Tubular Joint*. Offshore Technology Conference, Paper No. 5665, Houston.

Iida, K., 1987, *State of the Art in Japan*. Steel in Marine structures. Edited by Noordhoek, C., de Back., J, Elsevier Science Publishers B.V., pp. 71-98.

Inglis, C E. 1913, *Stresses in a Plate Due to the Presence of Cracks and Sharp Corners*, Proceedings, Institute of Naval Architects, Vol.60.

Irons, B.M. and Razzaque, A., 1972, *Experiments with the Patch Test for Convergence of Finite Elements*. Foundations of Finite Element Method with Applications to Partial Differential Equations, Academic press, pp. 557-587.

Irwin, G.R., 1957, *Analysis of Stresses and Strains Near the End of a Crack Traversing a Plate*. Transactions, ASME, Journal of Applied Mechanics, Vol.24.

Irwin, G.R., 1958, *Fracture*, Encyclopedia of Physics, Vol.6, Elasticity and Plasticity, pp. 551-590.

Klesnil, M. and Lucas, P., 1973, *Effect of Stress Cyclic Asymmetry on Fatigue Crack growth.* 1972. Material Science Engineering. Vol.9, pp. 231-240.

Kristiansen, M.O. and Fu, B., 1993, *The Free-Surface Stress Intensity Factor of Surface Cracks in Tubular Joint models.* Offshore Mechanics and Arctic Engineering, Vol.III-B, Materials Engineering, ASME pp. 795-801.

Kuang, J.G., Potvin, A.B. and Leick, R.D., 1975, *Stress Concentrations in Tubular Joints.* Offshore Technology Conference Paper, No.2205, Houston.

Kumar, V., German, M.D. and Schumacher, B.I., 1985, *An Analysis of Elastic Surface Cracks in Cylinders Using the Line-Spring Model and Shell Finite Element Method.* Journal of pressure Vessel Technology, Vol. 107, pp. 403-411.

Kumar, V. and German, M.D., 1985, *Studies of the Line-Spring Model for Nonlinear Problems* Transactions of the ASME, Vol.107, pp. 412-420.

Lawrence, F.V., Jr. 1980, *Predicting the Fatigue resistance of Welds.* Fracture Control Program Report No. 36, College of Engineering, University of Illinois at Urbana-Champaign.

Manson, S.S., *Discussion.* Trans. ASME, J. Basic Eng., Volume 84, No.4, pp. 533-537.

McGowan, J.J. and Raymund, M., 1979, *Stress-Intensity Factor Solutions for Internal Longitudinal Semi-Elliptical Surface Flaws in a Cylinder Under Arbitrary Loading.* Fracture Mechanics, C.W. Smith (editor) ASTM STP 677, American Society for Testing of materials, pp. 365-380.

Miyamoto, H. and Miyoski, T., 1971, *Analysis of Stress-Intensity Factors for Surface Cracked Tension Plate.* Proc. of Symposium on High Speed Computing of Elastic Structures, Leige, Belgium Vol.1, pp. 137-155.

Morrow, J., 1968, *Fatigue Properties of Metals.* Fatigue Design Handbook, Society of Automotive Engineers, pp. 21-30.

Munaswamy, K., Williams, P. and Swamidas, A.S.J., 1987, Fatigue Tests of unstiffened Tubular T-Joints, Progress report AMCA-DSS Project DS6 File No. 235Q.23440-4-9276 Serial No. 05Q84-00431, submitted to Materials Technology Centre, AMCA, Ottawa, 122 p.

Newman, J.C., Jr. and Raju, I.S., 1979a, *Analysis of Surface Cracks in Finite Plates Under Tension and Bending Loads*, NASA TP 1578, National Aeronautics and Space Administration.

Newman, J.C., Jr. and Raju, I.S., 1979b, *Analysis of Surface Cracks in Finite Plates under Tension and Bending Loads*. NASA TP 1578, National Aeronautics and Space Administration.

Newman, J.C., and Raju, I.S., 1981, *Fatigue Crack Growth Study of Residual Stress Effects*. International Journal of Fatigue 14, No. 4. pp.233-237.

Nwosu, D.I. 1993, *Fatigue Strength Analysis of Offshore Tubular Welded Joints Under Constant Amplitude Loading: Local Strain and Fracture Mechanics Approach*. Ph.D. Thesis, Memorial University of Newfoundland St. John's, Canada, pp. 285-290.

Pang, H.L.J., 1993, *Fatigue Crack Growth and Coalescence of Surface Cracks*. Offshore Mechanics And Arctic Engineering, Vol. III-B , Materials Engineering, ASME, pp. 485-491.

Paris, P. and Erdogan, F., 1963, *A Critical Analysis of Crack Propagation Laws*. Journal of Basic Engineering, Trans. ASME, Vol.85, pp. 528-534.

Parks, D.M., 1974, *A Stiffness Derivative Finite Element Technique for Determination of Crack Tip Stress Intensity Factors*. International Journal of Fracture, Vol.10, pp. 487-502.

Parks, D.N., Lockett, R. and Brockenbrough, J.R., 1981, *Stress-Intensity Factors for Surface Cracks in Plates and Cylindrical Shells using Line-Spring Finite Elements*. Proc. of the Winter Annual Meeting, ASME, Washington, D.C, pp. 279-285.

Parks, D.M., 1981a, *Inelastic Analysis of Surface Flaws Using the Line-Spring Model*. Advances in Fracture Research (ICF), Vol.5, pp. 185-194.

Parks, D.M., 1981b, *The Inelastic Line-spring Estimates of Elastic-Plastic Fracture Mechanics Parameters for Surface-Cracked Plates and Shells*. Journal of Pressure Vessel Technology, Vol.103, pp. 246-254.

Parks, D. M., and White, C. S., 1982, *Elastic Plastic Line Spring Finite Elements for Surface Cracked Plates and Shells*. ASME publication, Pressure vessel and piping Vol. 58

Pian, T.H.H. and Moriya, K., 1977, *Three-Dimensional Crack Element by Assumed Stress Hybrid Model*. Recent Advances in Engineering Sciences. Proc. of the 14th Annual Meeting, Bethlehem, PA, pp. 913-917.

Pian, T.H.H. and Moriya, K., 1978, *Three-Dimensional Fracture Analysis by Assumed Stress Hybrid Elements.* Numerical Methods in Fracture Mechanics, Proc. of The First International Conference, Swansea, Wales, pp. 363-373.

Pook, L.P, Kam, J.C.P. and Mshana, Y., 1992, *On Mixed Mode Fatigue Crack Growth in Tubular Welded Joints.* Offshore Mechanics and Arctic Engineering, Vol. III-B, Materials Engineering, ASME, pp. 251-255.

Raju, I.S. and Newman, J.C., Jr., 1977a, *Three-Dimensional Finite Element Analysis of Finite-Thickness Fracture Specimens.* NASA TL D-8414, National Aeronautics and Space Administration, 42 pages.

Raju,I.S. and Newman, J.C., Jr. 1977b, *Improved Stress-Intensity Factor for Semi-Elliptic Surface Cracks in finite Thickness Plates.* NASA TM X-72825, National Aeronautics and Space Administration, Washington, DC.

Raju, I.S. and Newman, J.C., 1977c, *Improved Stress-Intensity Factor for Semi-Elliptic Surface Cracks in Finite Thickness Plates.* NASA TM X-72825, National Aeronautics and Space Administration, Washington, DC.

Raju, I.S. and Newman, J.C., Jr., 1979a, *Stress-Intensity Factors for a Wide Range of Semi-Elliptical Surface Cracks in Finite Thickness Plates.* Engineering Fracture Mechanics, Vol.11, pp. 817-829.

Raju, I.S. and Newman, J.C., Jr., 1979b, *Stress-Intensity Factors for Two-Symmetric Corner Cracks.* Fracture Mechanics ASTM STP 677, American Society for Testing of Material, pp. 411-430.

Rhee, H.C., Han, S. and Gipson, G.S., 1991, *Reliability of Solution Method and Empirical Formulas of Stress Intensity Factors for Weld toe Cracks of Tubular Joints.* Offshore Mechanics and Arctic Engineering, Vol. III-B, Materials Engineering, ASME, pp. 441-452.

Rice, J.R. and Levy, N., 1972a, *Some Remarks on Elastic Crack Tip Stress fields* International Journal of Solids and Structures, Vol.8, pp. 751-758.

Rice, J.R. and Levy, N., 1972b, *The Part-through Surface Crack in an Elastic Plate* Journal of Applied Mechanics, Vol. 39, pp. 185-194

Ritchie, D. and Voermans, C.W.M., 1985, *Stress Intensity Factors in an Offshore Tubular Joint Test Specimen.* Proceedings of the Fourth International Conference on Numerical Methods in Fracture Mechanics. pp. 715-725.

Ritchie, D., 1986, Private Communication.

Schütz, 1981, *Procedures for the Prediction of Fatigue Life of Tubular Joints.* International Conference on Steel in Marine Structures, Paris, pp. 254-308.

Shah, R.C., and Kobayashi, A.S., 1972, *On the Surface Flaw Problem.* Physical Problems and Computational Solutions, ASME, pp. 79-124.

Shah, R.C., and Kobayashi, A.S., 1974, *Elliptical Crack in a Finite-Thickness Plate Subjected to Tensile Bending Loading.* Transactions ASME, Journal of Pressure Vessel Technology, Vol.96, pp. 47-54.

Skorupa, M., and Skorupa, A., 1993, *Significance of Crack Initiation Period in Structural Steel Welds.* Offshore mechanics and Arctic Engineering Vol. III-B Materials Engineering ASME pp. 715-720.

Sloane, S.W. and Randolph, M.F., 1983, *Automatic Element Reordering for Finite Element Analysis with Frontal Solution Schemes.* International Journal for Numerical Methods in Engineering, Vol.19, pp. 1153-1181.

Smith, F.W. and Alavi, M.J., 1971, *Stress-Intensity Factors for a Penny-Shaped Crack in a Half-Space.* Engineering Fracture Mechanics, Vol. 3, pp. 241-254.

Smith, F.W., 1972, *De-elastic analysis of the Part-Circular Surface Flaw Problem by the Alternating Method.* Physical Problems and Computational Solutions ASME, pp. 125-152.

Socie, D.M. Mitchell, R. and Cowfield, D. M., 1978, *Fundamentals of Modern Fatigue Analysis.* FCP Report, No. 26, University of Illinois, Urbana.

Tada, H., Paris, P.C., and Irwin, G.R., 1973, The Stress Analysis of Cracks Handbook, Del Research Corporation Hellertown, Pennsylvania.

Tong, P. and Atluri, S.N.. 1977, *On Hybrid Finite Element Technique for Crack Analysis.* Proc. Int'l. Conf. on Fracture Mechanics and Technology, Hong Kong, Sijthoff and Noordhoff Publishers, Vol.2, pp. 1445-1466.

Tos, H., Lambert, S.B. and Burns, D.J., 1993, *Fatigue Life Prediction for Welded Joints Under Variable Amplitude loading Using a Multiple Crack Model.* Offshore Mechanics and Arctic Engineering, Vol. III-B, Materials Engineering, ASME, pp. 697-707.

Tracey, D.M., 1974, *Finite Elements for Three-Dimensional Elastic Crack Analysis.* Nuclear Engineering in Design, Vol.26, pp. 282-290.

Tsang, A.A., 1981, *A Comparison of Three-Dimensional Finite-Element Solutions for*

the Compact Specimen. International Journal of fracture, Vol.17, pp. R125-R129.

Underwater Engineering Group, 1985, *Design of tubular Joints for Offshore Structures.* UEG Publications, URT 33.

van Straalen, I.J., and Dijkstra, O.D., 1993, *Prediction of the Fatigue Behaviour of Welded Steel and Aluminium Structures with the Fracture Mechanics Approach.* Paper to be Published in the Journal of Constructional Steel Research.

Williams, M.L., 1952, *Stress Singularities Resulting from Various Boundary Conditions in Angular Corners of Plates in Extension.* Journal of Applied Mechanics, Vol 19, pp. 526-528.

Williams, M.L., 1957, *On The Stress Distribution at the Base of a Stationary Crack* Journal of Applied Mechanics, Trans., ASME, Vol.24, pp. 109-114.

Wordsworth, A.C. and Smedley, G.P., 1978, *Stress Concentrations at Unstiffened Tubular Joints.* European Offshore Steel Research Select Seminar, Paper 34, Cambridge.

Wordsworth, A.C. and Smedley, J.P., 1978, *Stress Concentrations at Unstiffened Tubular Joints.* Lloyds Register of Shipping, London, European Offshore Steel Research Seminar, pp. 31.

Wordsworth, A.C., 1981, *Stress Concentration factors at K and KT Tubular Joints.* Proceedings, Fatigue in Offshore Structural Steel, Institute of Civil Engineers, Westminster, London, February, 1981.

Wu, S. and Abel, A., 1991, *Application of line-spring element in Analysis of Stress Intensity Factor and Fatigue Crack Propagation of Tubular Joints.* Int. Symp. Marine Structures, September, 12-15, Shanghai, China.

Wu, X.R., 1984, *Stress-Intensity Factors for Semi Elliptical Surface Cracks Subjected to Complex Crack Face Loading.* Engineering Fracture Mechanics, Vol.19, pp. 387-405.

Wylde, J.G. and McDonald, A., 1981, *Modes of Fatigue Crack Development and Stiffness Measurements in Welded Tubular Joints.* Paper 9 in Fatigue of Structural Steel, Conf. Organized by the Institution of Civil Engineering, London.

Yagawa, G. and Nishioka, T., 1980, *Superposition Methods for Semi-Circular Surface Crack.* International Journal of Solids and Structures, Vol.16, pp. 585-595.

Yagi, J., Machiada, S., Tomita, Y. and Matoba, M., 1991, *Influencing Factors on*

Thickness Effect of Fatigue Strength in As-Welded Joints for Steel Structures. Offshore Mechanics and Arctic Engineering, Vol. III-B, Materials Engineering, ASME, pp. 305-313.

Zienkiewicz, O. C., 1983, The Finite Element Method, McGraw-Hill and Sons, New York